Technical Report

Babcock & Wilcox Canada
Cambridge Ontario

"This report was prepared as an account of work sponsored by a Department of the Federal Government of Canada. Neither the Federal Government of Canada or any agency thereof, nor any contractor or subcontractor, nor any of their employees, makes any warranty, expressed or implied, or assumes any legal liability or responsibility for any third party's use of or the results of such use of any information, apparatus, product or process disclosed in this report, or represents that its use by such third party would not infringe privately owned rights".

WELD PROCESS DEVELOPMENT FOR FABRICATION OF HEAVY WALL PRESSURE VESSEL. PART 2

BY

B. WRIGHT,
BABCOCK & WILCOX CANADA

Work on this project was conducted under the auspices of the Canada Centre for Mineral and Energy Technology, Energy, Mines and Resources, Canada.

DSS FILE NUMBER:	213-121-000000-420502-0433
DSS CONTRACT SERIAL NUMBER:	OSQ-82-00145
CANMET PROJECT NUMBER:	1-9067-1
CANMET SCIENTIFIC AUTHORITY:	Dr. J. T. McGrath

OCT 11 1985
MICROMEDIA

79AP

CONTENTS

		PAGE
1.	SUMMARY	1
2.	INTRODUCTION	1
3.	PROGRAM OUTLINE	2
3.1	Primary and Secondary Variables	2
3.2	Test Assembly Design	2
4.0	PROCEDURE DEVELOPMENT	4
4.1	Comparison of Flux-Wire Combinations	4
4.2	Definition of Weld Groove Shrinkage	5
4.3	Effect of Manufacturing Variables	5
4.4	Welding Parameters for Capping Passes	6
4.5	Weld Repair Techniques	6
4.6	Effect of Welding Parameters upon Mechanical Properties	6
4.7	Optimisation of Welding Parameters	7
5.0	FULL THICKNESS WELDMENT	7
6.0	PRODUCTIVITY DATA	8
7.0	SUMMARY - WELD DEVELOPMENT PROGRAM	8
7.1	Comparison of Flux-Wire Combinations	8
7.1.1	Weldability Tests	8
7.1.2	Review of Chemical Analysis	9
7.1.3	Charpy V-Notch Data	10
7.1.4	Metallographic Examination	11
7.1.5	Selection of Flux-Wire Combination	12
7.2	Definition of Weld Groove Shrinkage	12
7.3.	Effect of Manufacturing Variables	13
7.3.1	Variable Root Gap	13
7.3.2	Variable Electrode Extension	14
7.4	Welding Parameters for Capping Passes	14
7.5	Weld Repair Techniques	15
7.6	Effects of Welding Parameters upon Mechanical Properties	15
7.7	Optimisation of Welding Parameters	16
8.0	SUMMARY - FULL THICKNESS WELDMENT	17
9.0	SUMMARY - PRODUCTIVITY DATA	19
10.0	DISCUSSION	20
11.0	REFERENCES	22

ABBREVIATIONS

A	Welding Current, Amps
AC	Alternating Current
BHN	Brinell Hardness Number
DC	Direct Current
DCEP	Direct Current, Electrode Positive
DCEN	Direct Current, Electrode Negative
ESO	Electrical Stick Out
HAZ	Heat Affected Zone
ISR	Intermediate Stress Relief
J	Heat Input, KJ/cm
LPE	Liquid Penetrant Examination
MPE	Magnetic Particle Examination
NDE	Non-Destructive Examination
N-GMAW	Narrow Gap Gas Metal Arc Welding
N-SAW	Narrow Gap Submerged Arc Welding
PWHT	Post Weld Heat Treatment
R	Range
RT	Radiographic Examination
S	Travel Speed, cm/min
SAW	Submerged Arc Welding
STC	Step Cool Heat Treatment
T	Interpass Temperature, °C
TS	Tensile Strength, MPa
TTr	Transition Temperature
UT	Ultrasonic Examination
V	Welding Voltage, Volts
WFS	Wire Feed Speed, cm/min
YS	Yield Strength, MPa

TABLES

TABLE		PAGE
1.	Reactor Vessel Weld Requirements	23
2.	Plate Material for Test Assemblies	24
3.	Welding Consumables for Flux-Wire Evaluation	25
4.	Results of Weldability Tests	27
5.	Effect of Welding Parameters Upon Mechanical Properties.	28
6.	Matrix of Welding Parameters for Procedure Optimisation.	29
7.	Plate Material for Full Thickness Assembly.	30
8.	Chemical Analysis of Filler Wire	31
9.	Chemical Analysis of Weld Deposit	32
10.	Comparison of Weld Deposit to Weld Wire Analysis	33
11.	Charpy V-Notch Test Results	34
12.	Effect of Notch Location on Weld Metal Toughness	35
13.	Etching Reagents for Macrostructure	36
14.	Dimensional Analysis of Narrow Groove Welds	37
15.	Shrinkage Data for 50mm Test Assemblies	38
16.	Dimensional Analysis of Narrow Groove Welds - Variable ESO	39
17.	Results from Optimisation Experiment.	40
18.	Effect of Chemical Analysis on Toughness.	41
19.	Welding Parameters for Full Thickness Assembly.	42
20.	Mechanical Tests Results for Full Thickness Assembly.	43
21.	Change in Calculated Deposition Rate with Welding Current.	46
22.	Flux Consumption Data	47
23.	Transverse Shrinkage for Full Thickness Assembly	48
24.	Weld Metal Analysis - Full Thickness Assembly	49

ILLUSTRATIONS

FIGURE		PAGE
1.	Test Assembly Design	50
2.	Hold Down Fixture Design	51
3.	Test Plate Design for Shrinkage Determination	52
4.	Test Assembly for Root Gap Evaluation.	53
5.	Detail of the ESAB Welding Head.	54
6.	Cross Section of Narrow Groove Weld	55
7.	Microstructure of Assembly 202	56
8.	Microstructure of Assembly 203	57
9.	Microstructure of Assembly 204	58
10.	Microstructure of Assembly 205	59
11.	Microstructure of Assembly 206	60
12.	Microstructure of Assembly 207	61
13.	Microstructure of Assembly 208	62
14.	Microhardness Survey	63
15.	Representation of Groove Wall Shrinkage and Distortion	64
16.	Relation of Groove Shrinkage to Depth of Weld.	65
17.	Distribution of Groove Shrinkage with Weld Length.	66
18.	Representation of Groove Distortion.	67
19.	Relation of Transverse Shrinkage to Weld Size.	68
20.	Effect of Weld Metal Oxygen Upon Toughness.	69
21.	Summary of Weld Dimensional Examination.	70
22.	Ferrite Veining in the Last Bead of Assembly 232.	71
23.	Cross Section through Full Thickness Weld	72
24.	Micro Hardness Survey through Full Thickness Weld	73

1.0 SUMMARY

The ESAB HNG Narrow Groove Welding System has been used in a laboratory environment to develop procedures for welding 2¼Cr-1Mo steel that satisfy petrochemical reactor vessel design. Manufacturing tolerances, repair techniques and parameters for capping passes have been established and the procedure has been demonstrated during welding, NDE and mechanical testing of a 203mm thick, 2.1m long assembly. Preliminary productivity data has also been collected.

Attempts have been made to rationalize the differences in Charpy toughness between the weld groove centreline and 1/4w locations. For 50mm weldments the 1/4w location shows inferior values whilst a reversal is noted in the full thickness assembly. The factors controlling toughness in 2¼Cr-1Mo weld metal are not clear although macrostructure and oxygen content appeared to be significant. Further work is necessary in this area because optical metallography does not resolve the diverse structures of the weld zone.

Weld groove shrinkage and distortion have been addressed but a predictive approach was not accurate for the full thickness assembly.

2.0 INTRODUCTION

The aim of the procedure development program was to establish submerged arc welding parameters that satisfy the mechanical property requirements defined in Table 1 and that produce, in a narrow preparation sound welds as defined by the NDE requirements of ASME Boiler and Pressure Vessel Code, Section VIII, Division 1. The attainment of mechanical properties after PWHT requires control of both the microstructure and the chemical analysis of the weld. To minimize the effects of temper embrittlement the approach taken was to maximize initial toughness and to limit trace elements by consumable selection.

The development program included the following tasks:

1. A comparison of commercially available flux-wire combinations to select one combination using weldability and toughness after PWHT as the acceptance criteria.

2. Definition of shrinkage in a narrow preparation to confirm weld groove dimensions.

3. Definition of the tolerance of the welding process to manufacturing variables i.e. joint misalignment.

4. Development of parameters to complete the weld groove capping passes.

5. Development of techniques for making repairs to the weld joint during production.

6. Evaluation of the effects of welding parameters, upon Charpy V-notch toughness and mechanical properties.

7. Optimisation of weld parameters in a narrow groove preparation using a partial parametric analysis with bead geometry and weld metal toughness as the acceptance criteria.

8. From the results of these tasks a 203mm thick assembly was welded and evaluated to ASME Boiler and Pressure Vessel Code Sections VIII and IX. Productivity data was collected during fabrication of this full thickness assembly.

3.0 PROGRAM OUTLINE

3.1 Primary and Secondary Variables

In SAW, the primary variables - welding current, voltage and travel speed - are governed by wire diameter, flux type and metallurgical considerations. The ESAB HNG head was developed for welding 3 or 4mm diameter filler metal in a nominal groove of 18mm. de Altama (1) has presented an optimised model of the N-SAW process in which an 18mm welding gap with a 2° included angle is welded with 500 to 700 amps DCEP using a 4mm diameter wire. Both European and Japanese fabricators favour a 4mm wire for N-SAW and this wire size was selected for this program. For a fixed wire diameter, the effects of varying welding current, voltage and travel speed upon weld metal properties and soundness were evaluated by maintaining secondary variables constant. The effects of the secondary variables (electrical stick-out, wire to sidewall angle, flux burden) were evaluated by separate experiments.

3.2 Test Assembly Design

The test assembly for flux-wire evaluation, optimisation of welding parameters and the evaluation of process parameters is shown in Figure 1. Anticipating that conditions would stabilize within 50mm of the weld start, the general test plate length was defined as 610mm to yield approximately 500mm of sound weld metal for evaluation. Plate thickness was defined as 50mm to ensure that 3D cooling conditions would be maintained over a range of heat inputs (2). The width of the plates were selected at 150mm to prevent edge effects upon cooling rate in the weld zone (2).

Test plate material was 2¼Cr-1Mo to avoid the effects of dilution. Chemical and mechanical properties of the plate material are recorded in Table 2. Plate material of the same grade for backing was not readily available and 1¼Cr-1Mo material was accepted in preference to flame cutting thicker and more expensive 2¼Cr-1Mo plate.

Preparation of the groove sidewall was intended to be a single 2° flame cut through each plate so that inverting one cut half would produce the

4° included angle recommended to accommodate weld joint shrinkage (1)(3). Trials were conducted to establish the reproducibility of flame cutting a 2° bevel using 1.8m long x 305mm wide x 50mm thick A36 plate. Transverse 2° flame cuts were made at 305mm intervals with a drive track, carriage and torch angle set independently for each cut. The flamecut surfaces of each experimental preparation were measured with a vernier protractor from the flame exit side of the plate at two locations along each face. The results were as follows:

	Side A	Side B
1st cut	1°	1° 40'
2nd cut	1° 15'	1° 50'
3rd cut	1° 40'	2° 30'
4th cut	2° 15'	3° 20'
5th cut	2° 30'	3° 15'

These results show that a 2° bevel on one side of the flame cut is not reproducible to better than ± 1° and that the matching faces of any one flame cut preparation are not consistent. The use of matching flamecut faces for the weld groove would not provide a 4° included angle, but one that varies from almost 3° to 6°. Accurately controlled angles on flamecut groove side walls of heavier gauge plate are difficult to produce and preparation of the 2° bevel angle was revised to a machining operation.

Preliminary tests were conducted to assess the degree of restraint required to minimize lateral distortion by using a 1.8m long, A36 assembly fabricated to Figure 1 with four equally spaced strong backs. 50mm gauge marks were used at 150mm intervals along the groove to measure joint shrinkage. The groove was welded using nominal parameters of 500A-30V-50cm/min travel speed. Distortion of the test assemblies resulted in the groove sidewalls becoming parallel. Most of the measured joint closure (80 percent) occurred with the joint half-filled. Since closure of the weld groove was accompanied by lateral distortion the experiment did not quantify real shrinkage. However, the strong back sizes were shown to be inadequate and were increased to 200mm deep by 75mm wide. To avoid repeated welding of large strong backs to each test assembly a welding jig was fabricated as shown in Figure 2. Tooling was also prepared to allow rapid fit-up of the root gap prior to tack welding the backing bar. The machined weld preparation was checked for bevel angle prior to assembly and each assembly was checked for root opening. Completed assemblies were stamped with a unique mark number prior to welding the groove.

Capping pass parameters were developed using flat 50mm plate and assemblies for proving repair techniques were produced from 200mm thick carbon steel plate.

4.0 PROCEDURE DEVELOPMENT

4.1 Comparison of Flux-Wire Combinations

Commercial flux-wire combinations were ordered from six manufacturers using the following purchasing details.

(a) One coil with liner of 4mm diameter submerged arc welding wire to AWS 5.23- Class EB3. Chemical composition to comply with the following restrictions (4):

Carbon	0.10 to 0.14 percent	Silicon	0.10 percent max.
Manganese	0.45 to 0.70 percent	Sulphur	0.12 percent max.
Phosphorus	0.12 percent max.	Copper	0.10 percent max.
Arsenic	0.01 percent max.	Tin	0.005 percent max.
Antimony	0.005 percent max.		

Elements Nickel, Aluminum and Vanadium are to be reported for information.

(b) 25 kg submerged arc welding flux to AWS 5.23 Class F82-EB3-B3. The flux shall be supplied in metal cans with resealable lids or in comparable containers that minimize contamination.

The flux-wire combinations are required for welding 2¼Cr-1Mo steel using a DCEP narrow groove SAW procedure. Weld material will be subjected to the Socal step-cool temper embrittlement simulation and shall show 54J Charpy V-notch toughness at -29°C.

The flux-wire combinations received are listed in Table 3 together with measured characteristics of both wire and flux.

Seven test assemblies were welded with these consumables using standard welding parameters of 550A-30V-50cm/min travel speed, a preheat temperature of 200°C and an interpass temperature of 300°C. During welding, characteristics as defined in Table 4 were monitored and rated using the numerals 1, 2 and 3 to represent good, average and poor respectively. Groove wall shrinkage was measured across the groove using 50mm gauge marks and root shrinkage was monitored adjacent to the weld start and stop locations.

Each completed assembly was given a PWHT for 8 hours at 690°C using a maximum heating and cooling rate of 55°C per hour. Five Charpy V-notch specimens were removed from the weld with the notch located perpendicular to the weld face at the groove mid-width; the long axis of the specimen was located at the groove mid-thickness. Charpy V-notch results were rated in a similar way to weldability; absorbed energy values less than 54J were rated with 4; 54 to 81J was rated 3; 81 to 102J with a 2 and above 102J rated at 1. Chemical analysis was performed on each filler wire received and on each weld metal using samples removed by drilling along the weld centreline and 6mm above the backing bar.

Cross sections of each welded assembly were prepared for both macroscopic and microscopic examination using standard metallographic techniques.

4.2 Definition of Weld Groove Shrinkage

Preliminary values for narrow groove shrinkage were obtained from the test assemblies used to evaluate flux-wire combinations (Section 4.1). The results obtained were disappointing since significant lateral distortion occurred (Para. 7.2). A literature search was conducted to identify published data for joint shrinkage but information pertinent to the N-SAW process was not found. More elaborate tests were therefore devised to quantify groove shrinkage and to estimate the sidewall angles required for a 200mm thick weld joint. 2¼Cr-1Mo steel plates were machined to give flat, 330mm wide by 810mm long test plates with a 10mm root radius, 4° included angle weld groove. Assemblies were 50, 100 and 150mm thick (Figure 3). The plates were bolted to a flat rigid jig to minimize lateral distortion, preheated to 150°C and welded at 550A-32V-50cm/min travel speed. Transverse shrinkage at the face of the groove was measured with vernier calipers after each layer using 50mm gauge lengths across the groove.

4.3 Effect of Manufacturing Variables

The narrow groove weld root opening recommended by ESAB is nominally 19mm. To establish the limits to root gap that the ESAB head would tolerate the test assembly shown in Figure 4 was prepared with the root varied from 15mm to 25mm over a length of 915mm. The groove was welded using 150°C preheat, 550A-30V-55cm/min travel speed. The welding head was guided from one sidewall with no attempt made to correct for the variation in groove width. The soundness of the completed weld was assessed by radiographic plus ultrasonic examination, sidebend tests and examination of macrosections.

The ESAB HNG head (Figure 5) is constructed so that the contact jaw assembly swivels approximately 105mm above the end of the blade. The electrical stick-out (ESO) is increased by adjusting the height sensing probe so that the complete head is raised in the groove. Raising the head also results in an increase in the flux feed nozzle to root distance and therefore an increase in flux burden. Since the contact jaw assembly swivel point is raised, small decreases in the wire to sidewall angle also occur.

Conventional SAW uses electrical extensions of 40mm and values of 40, 48 and 54mm were selected for trials. Over this range of ESO the calculated wire to wall angle was 2.8, 2.7 and 2.6 degrees respectively and flux burden increased from 6 to 14 to 20mm respectively. Standard test assemblies (Figure 1) were welded with the three ESO values and no adjustment to wire feed speed or power source output was required to maintain constant welding parameters of 550A-30V. Travel speed was 55cm/min. Test welds were evaluated upon completion by macroscopic examination of cross sections including dimensional examination of bead shape and penetration.

4.4 Welding Parameters for Capping Passes

Welding parameters were established by trial and error using bead on 2¼Cr-1Mo plate tests to produce flat beads suitable for groove completion. Weld beads were assessed by visual examination, macroscopic examination of cross sections and by bend tests. Whilst ASME Boiler and Pressure Vessel Code, Section VIII permits reinforcement of welded seams, tighter limits are placed on the bead height above the plate by the needs of radiographic and ultrasonic examination methods. The final confirmation of capping pass parameters would be an acceptable profile for MPE and RT during examination of the full section assembly.

4.5 Repair Techniques

The successful use of N-SAW requires an ability to remove defective weld material and execute repairs without significantly changing the weld preparation. Conventional repair techniques i.e. hand grinding, carbon arc gouging are not appropriate to a narrow groove preparation in thick sections. The use of high speed grinding was selected as a practical method for removing weld metal prior to groove completion.

A 150mm thick carbon steel assembly with a 20mm root opening and a nominal 4° included angle was welded to approximately quarter depth using welding parameters of 500A-30V-55cm/min travel speed and a 48mm ESO. The partially filled groove was subjected to a repair cycle in which imaginary sidewall defects were removed by grinding. Equipment used for defect removal was a high speed grinding head supported by a manipulator. This equipment is manufactured by Voka Company in Switzerland and has been successfully used for back grinding conventional weld seams. A 660mm dia. grinding wheel was dressed from 20mm to 18mm thickness to accommodate the narrow groove preparation and rotated at 1760 rpm to remove "defective" weld metal over a predefined length and depth without removing more than 0.8mm from one sidewall. Welding of the groove was completed over the repaired area. The completed weld was subsequently ground at the root and face and subjected to the radiographic plus ultrasonic examination.

4.6 Effect of Welding Parameters Upon Mechanical Properties

Five standard assemblies (Figure 1) were welded using the parameters in Table 5 to evaluate the effect of heat input and interpass temperature upon toughness and tensile properties. The welded assemblies were subjected to MPE, RT and UT inspections prior to a PWHT cycle of 20h at 690°C. Charpy V-notch specimens were removed from the weld metal at the 1/4w location and from both base metal and heat affected zone at the 1/4t location. All weld metal tensile specimens (12.5mm standard round) were removed at the weld mid-depth and tested at room temperature.

4.7 Optimisation of Welding Parameters

In order to establish limits to welding parameters that produce acceptable weldments, a partial parametric experiment was devised that involved nineteen standard assemblies (Figure 1) welded in the sequence and with the parameters indicated in Table 6. Weld quality was assessed by metallographic examination for bead depth to width ratio, sidewall penetration, degree of recrystallization of previous weld beads; incidence of cracking, lack of fusion, porosity and undercut; hardness, microstructure and Charpy V-notch toughness at -40°C.

5.0 FULL THICKNESS WELDMENT

Material for the full thickness assembly was 203mm thick SA387 Gr22 Cl2 plate. Table 7 summarizes the mechanical and chemical properties of the material provided by the vendor. A section of the plate was removed and machined to provide an ASME Boiler and Pressure Vessel Code, Section V calibration block for subsequent ultrasonic examination of the weld.

The plate was flame cut to give two pieces 305mm wide x 2.1m long which were subsequently machined flat and bevelled with a 1 degree weld preparation. Magnetic particle examination was performed on the preparation sidewalls to confirm an absence of laminations.

The groove was welded using the parameters in Table 19. Backing bars and strong backs were removed and the root area ground in preparation for radiographic examination. Standard radiographic techniques in accordance with ASME Boiler and Pressure Vessel Code, Section V were used initially to evaluate the welded assembly without grinding the weld face. The source of radiation was a 4MeV linear accelerator, source to film distance 1.8m and film type Kodak AA. Radiographic examination was repeated using high resolution film (Kodak M).

Following radiographic examination the weld face was locally ground in preparation for magnetic particle and ultrasonic examinations. Standard ultrasonic examination in accordance with ASME Boiler and Pressure Vessel Code, Section V was performed using pulse echo, 45° and 60° angle probes plus normal beam inspection from one surface. These techniques were supplemented by a 45° tandem probe examination from both root and face. Magnetic particle examination of both root and face surfaces was performed using the DC yoke method.

PWHT of the full thickness assembly was achieved in a production oil-fired furnace in one cycle at 690°C ± 10°C with a hold period of 20h. Heating and cooling rates above 315°C were controlled at 55°C/h. The complete thermal cycle was monitored by thermocouples attached at three locations along the weld length and connected to a strip chart recorder.

Samples for mechanical testing were sawcut transverse to the weld long axis. Two reduced section tensile test specimens and four transverse sidebend test specimens were prepared in accordance with ASME Boiler and Pressure Vessel Code, Section IX. Each tensile test was cut into two

specimens and each bend test cut into four specimens to accommodate the full thickness of the weld. Standard Charpy V-notch specimens were removed to evaluate the base metal, HAZ, and weld metal at locations 1.6mm below the surface, 1/4t and 1/2t below the surface; test temperature was -40°C. Specimens were also removed from 3/4t below the surface in the three zones and tested at -29°C for information. All weld metal Charpy specimens were duplicated to test both the 1/4w and 1/2w locations. Charpy specimens from the heat affected zone were located as close as practical to the fusion line. Prior to notching, each Charpy specimen was checked to confirm the notch location and after machining each specimen was dimensionally inspected (shadowgraph) to confirm notch accuracy to ASTM A370 requirements.

Chemical analysis of the weldment was performed on drillings taken through the depth of the weld. Microhardness surveys were conducted at 1.6mm , 1/4t, 1/2t and 3/4t locations below the surface of the weld.

6.0 PRODUCTIVITY DATA

Consumable useage and welding times were monitored during welding of the full thickness sample. To supplement this data, wire feed speeds were measured at each of the welding current values used during the procedure optimisation experiment to produce deposition rate data.

In order to define flux consumption rates, bead on plate welds were made using welding parameters from the optimisation experiment. Flux delivery per unit length was established for each set of parameters prior to welding and flux consumption calculated by difference after welding each bead. From these results plus deposition rate data theoretical flux to wire consumption ratios were calculated.

Transverse shrinkage was measured during welding of the full thickness assembly using 50mm gauge marks across the face of the weld groove.

7.0 SUMMARY - WELD DEVELOPMENT PROGRAM

7.1 Comparison of Flux-Wire Combinations

7.1.1 Weldability Tests

All wires received were copper coated, but showed varying degrees of brightness and surface oxidation (tarnish). In spite of the various ratings attributed to each wire (Table 4), no significant difference was noted by a white paper wipe test; all wires showed a similar pick-up of brown/black oxides. The cast and helix for each wire were normal except for the Oerlikon wire which showed an excess helix; wire feed for this product was rated normal.

Uniform feeding of Linde 124 flux was attained with increased air pressure, however, the excess pressure resulted in unused flux being transferred to the dust collector. The flux feed recovery system did not operate satisfactorily with fused fluxes but would operate with the dust collector disengaged. The Kobe flux being extremely fine (48 x D) also required increased air pressure to feed uniformly which again resulted in flux losses to the dust collection system. The slag produced by the Kobe consumables was not self-peeling although improved performance may result with revised parameters. Weld appearance with the Linde products was irregular showing beads of varying height, characteristic of high amperage. Undercut was not visually evident in any of these test assemblies. A sputtering arc and intermittent combustion of gases above the flux was noted with the Thyssen consumables.

7.1.2 Review of Chemical Analysis

Chemical analyses of wire samples are shown in Table 8 and of weld samples in Table 9.

Carbon (0.10 to 0.13 percent) and Manganese (0.4 to 0.8 percent) contents are not significantly different between wires and all consumables were expected to show equivalent strength values. No serious deviation from the requested ranges were noted. Significant differences were noted for Silicon content which varied from 0.08 to 0.21 percent; only the wire from Kawasaki complied with the 0.10 percent maximum.

The high purity required to minimize temper embrittlement is reflected in Phosphorus levels (general 0.006 percent) except for the Linde and Oerlikon products (0.012 percent). Sulphur levels in all samples were less than 0.010 percent. Elements of secondary importance to temper embrittlement response were also uniformly low i.e. 0.006 maximum Tin, 0.003 maximum Antimony and 0.005 maximum Arsenic. Variations were noted in Nickel, Vanadium and Aluminum contents.

Chemical analysis of weld deposits were compared to the corresponding wire analysis and the percentage change in composition recorded in Table 10. Data for the Oerlikon products has not been included since the original analysis was obtained from an undiluted weld deposit. All but the Kawasaki consumables showed a Carbon content decrease of 20 to 60 percent during welding. For DCEP submerged arc welding such losses are normal and the slight increase in Carbon content for the Kawasaki weldment is attributed to experimental error rather than a reversal of the Carbon loss trend. All but the Kobe consumables showed a Manganese increase of 20 to 60 percent. The small loss in Manganese for the Kobe weldment again is attributed to experimental error rather than a trend reversal. Silicon transfer in all weldments was positive, but a large variation is noted i.e. +20 to +230 percent. This variation was not related to Manganese increases and reflects the variation in flux activity. Chromium and Molybdenum losses are uniform at 5 to 10 percent. The variable changes in Antimony, Tin and Arsenic are small and are probably related to experimental error in analysis. Certainly no

significant cleaning action of the flux is indicated with any consumable combination and a trend to increase in Arsenic is indicated. For the Kawasaki product a positive change in Vanadium is noted which arises from the intentional ferro-vanadium additions in the flux formulation.

Chemical analysis of all deposits except that from the ESAB Consumables comply with AWS 5.23 EB3 requirements; the ESAB deposit analysis shows slightly less than the 0.90 percent minimum for Molybdenum.

7.1.3 Charpy V-Notch Data

Test assemblies were welded with nominally the same heat input, interpass temperature and weld preparation and the PWHT cycle was identical so that chemical factors were considered to be the essential variable to Charpy V-notch toughness. The values shown in Table 11 show poor correlation with weld metal oxygen centent and purity factors.

Considerable scatter in Charpy impact energy and lateral expansion is noted within any one set of five specimens. The scatter in values does not correlate with average values of absorbed energy as shown below:

Assembly	Average Toughness, J	Scatter in Absorbed Energy, J	Scatter in Lat. Exp., mm
207	27	24	0.30
202	32	65	0.64
205	38	24	1.25
206	89	7	1.03
204	96	35	1.48
208	110	24	1.36
203	116	128	1.40

The macrostructure of the narrow groove weld (Figure 6) consists, at 1/2w, of overlapping zones of non-columnar weld metal and at 1/4w of alternate layers of columnar zones and weld metal heat affected zone. Three assemblies were tested at both locations to establish whether the scatter at 1/2w was the result of variation in notch location and to establish both average value/scatter in properties at 1/4w. The repeat test results (Table 12) at 1/2w showed average and scatter values similar to the initial tests. These results together with metallographic examination of broken impact specimens confirmed that notch mis-location was not the cause of Charpy V-notch scatter.

Data from Kobe Steel (5), Kawasaki Steel (6) and Thyssen Draht (7) shows that -40°C represents the lower transition region for 2¼Cr-1Mo weld metal where scatter in absorbed energy is normally noted. Tests results for single bead per pass welds show scatter in absorbed energy at -40°C of between 67 and 94J so that scatter in the results in this work may be considered normal.

The average values of absorbed energy at 1/4w were lower than at 1/2w and below or borderline compared to the acceptance criterion (54J at -40°C). A somewhat lower scatter in absorbed energy is noted at 1/4w. Subsequent tests were conducted at this weakest link location.

7.1.4 Metallographic Examination

Figure 6 shows a typical macrosection through a 50mm thick weld. The groove filling technique of depositing beads at alternate sidewalls results in partial recrystallization of previous beads in the through-thickness direction and a central recrystallized band at the groove mid-width. Definition of the macrostructure of stress relieved (tempered) sections was attempted using reagents on surface ground and polished surfaces with the most detailed structure being developed with a hot HCl/50% H_2O reagent. The complete list of etchants evaluated are listed in Table 13.

Cross-sections from each assembly were dimensionally examined to compare the refined and unrefined fractions at 1/4w. Using a line intercept method the depth of the two zones was measured at a magnification of 10X and results summarized in Table 14. The relatively small differences noted between bead depth values are attributed to the extent of groove filling prior to depositing the capping passes. The variation noted for the ratio of refined to unrefined structure between the weld assemblies is significant since the depth of bead and heat affected zone at 1/4w were expected to be similar using the same welding parameters. Factors which contribute to this variation include the difficulty experienced in identifying the extent of the refined zones owing to poor etching response and the statistical variation in penetration and heat affected zone size at nominally constant welding parameters. Bead on plate welds at 550A-30V-50cm/min travel speed sectioned at 100mm intervals showed the following variation in bead contour:

Preheat	Bead Width (mm)	Bead Depth (mm)	HAZ Width (mm)
21°C	17.7 to 18.2 Mean = 17.9	6.8 to 7.4 Mean = 7.1	0.8 to 1.0 Mean = 0.9
93°C	18.9 to 19.8 Mean = 19.4	7.0 to 7 6 Mean - 7.3	1.6 to 1.9 Mean = 1.7
150°C	18.0 to 19.2 Mean = 18.6	6.8 to 7.4 Mean = 7.0	1.2 to 1.4 Mean = 1.3

Additionally, adjustments were made to the welding head location and wire to wall distance during welding. Variation in root gap along each test assembly and in sidewall angle at both sides of the groove was permitted during manufacture of the test assemblies. Since the location of the weld head was referenced to one sidewall by the horizontal probe the location of the head and the wire to wall distance required correcting as

groove filling progressed in order to uniformly weld against the second sidewall. This resulted in bead placement that was not standard at each alternate sidewall and therefore a variation in bead profile is applicable. Additionally, the height sensing probe references the head from a uniform surface only for the root beads. Thereafter, the height of the head was referenced to a variable fillet weld surface. Subsequent weld assemblies were made with the welding head centred for each layer but without adjustment of the wire to wall distance.

Although low temperature toughness was expected to be related to macrostructure, no correlation of Charpy V-notch toughness at 1/4w and the ratio of refined to unrefined structure has been found.

Representative microstructures from each assembly are shown in Figures 7-13. The microstructure is tempered bainite with an absence of pro-eutectoid ferrite. No significant difference is noted apart from prior austenite grain size between the coarse and refined regions.

Knoop microhardness surveys were conducted across each section and along the centre refined region. Results are shown in Figure 14 and confirm that after eight hours PWHT at 690°C the maximum hardness is below the 215 BHN acceptance criterion.

7.1.5 Selection of Flux-Wire Combination

The overall assessment attributed to the flux-wire combinations (Table 4) shows that Oerlikon, Thyssen and Kawasaki have provided preferred consumables. The Oerlikon weld wire was considered third choice because of its flux-core manufacture; consistent properties would be not only dependent upon welding parameters but also upon consistency of flux filling. The toughness values obtained with the Kobe Steel combination were higher than for the Thyssen Draht combination but the latter material was selected for all subsequent test welds on the basis of delivery time.

7.2 Definition of Weld Groove Shrinkage

The values for joint shrinkage measured during welding the 50mm thick assemblies used for flux-wire evaluation are recorded in Table 15. The results are of limited value for estimating weld preparation requirements since they represent groove shrinkage plus reduction in groove width due to lateral distortion which was evident even though 135Nm of torque was applied to the hold down bolts. Measurement of lateral distortion was approximate because alignment of the plates in each assembly was not precise. Shrinkage across the gauge marks is shown schematically in Figure 15 as a reaction to lateral distortion only. Using the data from Assembly 208 (Table 15) the angular distortion, "b" is approximately $\tan^{-1}$ 2.03/152 = 0.77° and the apparent shrinkage at the weld face Δ G is the sum of 2 (50.8 tan 0.77°) plus the measured root closure i.e. Δ G = 2.12mm. Using this approach the measured shrinkage across the groove face is approximately equal to root closure plus lateral distortion.

Transverse shrinkage measured across the machined test assemblies (Figure 3) increased continuously during welding as shown in Figure 16, which represents measurements at the plate mid-length. The initial groove shrinkage is rapid but transverse shrinkage along the weld shows a maximum at the plate mid-length with reduced values at the start and stop locations (Figure 17). This distribution of results agrees with the description of distortion given by Leggatt (13).

Transverse shrinkage of each groove was accompanied by lateral distortion of the plate. The extent of distortion is summarized below for both top and bottom surfaces of each plate as a deviation from the original flat condition.

Test Plate Thickness (mm)	Maximum Shrinkage (mm)	Transverse Distortion Top Surface (mm)	Bottom Surface (mm)
50	1.5	0.44	n/a
100	3.5	1.98	0.96
150	5.8	2.50	1.59

The effects which contribute to changes in the geometry of a weld preparation in flat plates is summarized in Figure 18. The measured transverse distortion is shown by calculation to have a negligible effect upon measured shrinkage and the effect of root shrinkage, S_o, is assumed to be negligible. Ohsawa et al (14) have shown for N-GMAW preparations that S_o is small and constant after the first 20mm of weld has been completed. The plates welded in the current experiment were machined with a 10mm integral backing so that errors introduced by neglecting S_o are small.

Figure 19 relates measured values from groove shrinkage to plate thickness which predicts a shrinkage of 7.9 mm for a 200mm plate. Linear extrapolation does not include the restraining effect of the weld ligament which resists bending. Alternate relationships between shrinkage and groove cross-section (Figure 19) predict a shrinkage of 8.0mm for a 200mm plate or an angular distortion of $\tan^{-1}(4.0/203) = 1.13°$. As a further check on groove closure the angular distortion values calculated in Figure 18 are related in Figure 19 to plate thickness and extrapolation predicts an angular distortion of almost 1.2°. Recognizing that the data presented ignores root shrinkage, transverse distortion and root collapse that may occur in production, weld preparations for a 200mm assembly were specified at 1 to 1.5°, that is a 2° to 3° included angle.

7.3 Effect of Manufacturing Variables

7.3.1 Variable Root Gap

The width of the flux feed nozzle (see Figure 5) sets the minimum width into which the head will enter at 14mm. Centralizing the welding head in the groove mid-length (Figure 4) and then travelling toward the narrow

end maintains the wire to wall distance at 2.4mm from the referenced sidewall, but travel is restricted by interference of the feed nozzle with the non-referenced sidewall at point "A". Commencing to weld at this point does not immediately produce sound weld metal since the weld start position will continuously move toward the mid-length with successive beads in a flat plate. Hence, for a longitudinal seam the minimum width which can be welded is estimated at 19mm (B). For a circumferential seam the minimum width which can be welded is estimated at 18.5mm. Sidebends and macrosections removed at location "B" showed no lack of fusion defects. The upper limit to groove width which is bridged by the fillet welds at alternate sidewalls was noted visually during welding at point "C" (22.5mm wide). The incidence of lack of fusion during ultrasonic and radiographic examination beyond this point confirmed the visual observations. Macrosections and sidebend tests showed no lack of fusion defects at location "C".

The results of this experiment indicate that for practical applications the range of root opening that can be welded with two beads per pass to produce sound weld metal is 19 to 22mm.

7.3.2 Variable Electrode Extension

The effects of varying ESO was evaluated using Thyssen welding consumables. Welding with an ESO of 40mm produced intermittent open arcing and spatter as a result of low flux burden. With an ESO of 54mm, excessive flux build-up was apparent but arc stability was good. An ESO of 48mm provided good flux coverage and arc stability and was selected for further procedure development.

Macroscopic examination of cross sections removed from the three assemblies yielded the dimensional analysis reported in Table 16. Bead depth (penetration) increases slightly and the depth of refined metal is reduced as ESO increased. Variation in depth of non-refined weld metal and sidewall penetration showed poor correlation with increases in ESO. These observations require consideration in light of the ESAB voltage and amperage control circuits. Normally, increasing ESO results in a fall in welding current because of I^2R heating losses and unless wire feed speed is increase, penetration will fall with increase in ESO. The ESAB voltage regulation circuit and the electrode feed unit clearly held these parameters constant during these tests since no adjustments were necessary to maintain welding parameters. Thus the changes in bead depth (penetration) and depth of HAZ (refined weld metal) may not be significant. The depth of sidewall penetration does not relate to ESO nor therefore to concurrent changes in wire to wall angle.

7.4 Welding Parameters for Capping Passes

Welding parameters were established by trial and error using bead on plate (2¼Cr-1Mo) tests to produce flat beads for groove completion. Welding consumables from Thyssen Draht were used for this evaluation.

Commencing with standard weld parameters, (550A-30V-50cm/min travel speed) twelve (12) beads were deposited using increased voltage and reduced travel speed to flatten the bead contour. Parameters selected

for capping passes were approximately 550A-34V-30cm/min travel speed with a zero bead overlap. Examination of macrosections through these welds showed an absence of weld bead or heat affected zone cracking. Bend tests were acceptable to ASME Boiler and Pressure Vessel Code, Section IX standards.

7.5 Weld Repair Technique

The partially completed weld groove described in Section 4.5 showed a slight step at one sidewall after grinding the repair cavity indicating that the grinding wheel was not dressed exactly to the groove contour. The step was small - 9mm high from the ground cavity root and 0.7mm wide. The step was not removed prior to continuing the weld. With a machined weld preparation this step could be eliminated by using a more precisely matched grinding wheel but subsequent examination of this repair cavity suggests that extra precautions are not necessary.

Welding was continued over the ground area without attempting to adjust the head or parameters to accommodate the groove dimension change.

Groove wall shrinkage of this assembly did not occur as expected after filling to t/3. This was attributed to the greater than optimum sidewall angle prepared by flamecutting (actual sidewall was 2° 30 min.). Parameters were revised to bridge the wall at t/3 and at 3/4t, three beads per pass were deposited. The completed weld was subsequently ground at the root and face and subjected to the radiographic plus ultrasonic inspection. The results of these examinations were acceptable to ASME Boiler and Pressure Vessel Code Section VIII acceptance criteria.

7.6 Effect of Welding Parameters Upon Mechanical Properties

The test assemblies were welded using 4mm dia. Thyssen S1CrMo2 wire (Heat 537183) with UV 420 TTR flux (Lot 367508).

Upon completion of welding the five test assemblies and prior to PWHT, magnetic particle examination of the face and root surfaces showed a continuous line of diffuse indications along the base metal and weld metal heat affected zones. Liquid penetration inspection of both surfaces showed an absence of indications. Microsections removed from these regions showed an absence of defects associated with the MPE indications which were therefore confirmed as non-relevant (i.e. resulting from metallurgical or permeability differences within the heat affected zones). Radiographic and ultrasonic examination of these plates were acceptable to ASME Boiler and Pressure Vessel Code, Section VIII requirements.

Referring to Table 5, tensile properties were not affected by either heat input over the range 17 to 22 kj/cm or interpass temperature over the range of 150 to 260°C. TS, YS and ductility values are above the minimums for SA387 Gr22 Cl2 plate. Comparison to the requirements for weld material is not strictly appropriate since the acceptance criteria of SFA 5.23 are for a PWHT at 690°C for one hour only. However, the data shows acceptable YS and ductility values with borderline TS values.

HAZ toughness values are all in excess of the values measured for the base material. Charpy V-notch values for the HAZ welded at low heat input are notably higher than at higher heat inputs. Significant scatter is evident in the Charpy V-notch data in spite of deliberately locating the notch parallel to and half the notch width from the fusion line.

Charpy V-notch values at -40°C for all weld metal 1/4w locations showed both a high degree of scatter and failure to meet 54J. No discernable effect of heat input or interpass temperature was apparent. Data from the optimisation experiment (Table 17) suggests that assembly #240 and 243 would contain a totally refined weld structure at 1/4w and assemblies #242 and 244 less than 50% grain refinement. Absorbed energy values are not significantly different as a result of grain refinement.

In attempt to clarify the effect of grain refinement upon toughness, three assemblies (222, 223, 224) from the optimisation experiment with 100 percent recrystallized weld metal were subjected to the same PWHT cycle and Charpy tests were removed at 1/4w. These results are summarized in Table 5 and gross variations in toughness are noted.

Broken Charpy specimens were metallographically examined in an attempt to establish the reason for low, intermediate and high values from weldments made with nominally identical welding parameters. Cross sections showed that the initial 100 percent recrystallization assessment was inaccurate, but no significant differences were measured in the amount of columnar weld metal along the notch of the 3 Charpy specimens. Comparison of results from assembly 222 and 223 suggest that increasing interpass temperature may be detrimental to weld metal toughness. Toughness of assembly 224 at 1/4w was acceptable and these parameters were selected for welding the full thickness assembly.

Chemical analysis of these assemblies is summarized in Table 18 from which no obvious trend relating chemistry to toughness is noted. Compared to the initial weld metal analysis, (see Table 9, assembly 203), Manganese content is slightly low, but Sulphur, Phosphorus and Oxygen levels are significantly higher. No explanation for the increases is available at present. Correlation of Charpy toughness at 1/4w location with Oxygen content was considered since -40°C represents the lower transition regime; Figure 20 indicates a trend towards higher toughness at lower Oxygen contents.

7.7 Optimisation of Welding Parameters

Results from the matrix of nineteen assemblies are summarized in Table 17 together with experimental data obtained from later test assemblies. Figure 21 shows schematically the areas measured and recorded. All assemblies were welded with Thyssen Draht welding consumables of the same wire heat and flux lot numbers (see Table 3).

Experimental results from assemblies 212, 221, 230 plus 241, all of which were welded using the reference welding parameters, are consistent when compared to the variation noted for bead on plate tests. (Section 7.1.4) The variation in depth of the top bead in each assembly from one side wall to the other is related to preparation of the test assemblies. The sidewall angles were not consistently 1° and root gaps were not

consistently 19mm so that weld beads deposited at alternate sidewall were not identical. Small variations in bead height, therefore, account for significant variations in dependent observations such as sidewall penetration and degree of recrystallization of previous beads. Bead depth at the guided sidewall increases with increase in amperage over the range of 450-550-650 amps although bead width shows no obvious change. Sidewall penetration shows poor correlation with amperage. The ratio of recrystallized to coarse weld metal in Table 17 was obtained using a line intercept approach at 1/4w. An average value was attributed to each zone and the function F/F+C calculated. Generally, the degree of recrystallization increases as the welding current decreases.

All weld sections showed minor porosity typically up to 10 pores per section, between 0.1 and 0.2mm in diameter. Rating each assembly on the basis of porosity content would involve both an assessment of size and volume and would be of questionable value. Porosity is therefore, not included in the assessment. Assemblies welded at 650 amps showed the lowest incidence of porosity. All samples showed an absence of sidewall undercut, weld zone cracking and lack of fusion defects.

Metallographic examination of all samples characterized the weld structure as bainitic but grain size differences could not be discerned between the columnar and refined zones. The top beads in each assembly exhibit narrow light etching veins which followed the general columnar growth patter (Figure 22). This constituent was identified by etching techniques and by elemental distribution as ferrite. Isolated veining was noted within the groove; the reduced incidence of ferrite within the groove attributed to heat treatment by successive beads. In Table 17 the incidence of ferrite veining is recorded as it would relate to toughness i.e. 0% if present in the top beads only, 100% if present in all beads throughout the groove depth.

A significant observation from Table 17 is that Charpy toughness at 1/4w complies with 54J at -40°C for only one test assembly after 20h PWHT at 690°C. Assembly 224 exhibits a completely recrystallized macrostructure, i.e. an absence of residual columnar weld metal, and shows 73J at 1/4w but several other assemblies also show 100% recrystallized weld metal with borderline toughness values.

Further cross-sections were removed from the nenteen assemblies and examined to increase the accuracy of the data in Table 17. Characterization of the macrostructure continued to be difficult because of the poor etching response of the columnar and recrystallized weld metal. The repeat examination was therefore terminated and the accuracy of the data was considered inadequate to pursue the intended statistical analysis.

8.0 SUMMARY - FULL THICKNESS ASSEMBLY

Magnetic particle examination of the machined groove sidewall showed an absence of indications. Fit-up of the assembly was accepted after the

9.5mm backing bar and the eight, 200mm deep x 75mm thick equidistant strong backs were attached, the root gap along the length measured 18-18-18.5mm with an included angle varying from 1° 45' to 1° 50'.

During welding, the bead appearance of the first five layers was poor and slag removal was more difficult than normal. Both observations were attributed to the relatively tight root gap. Slag removal and bead appearance continually improved as the groove was filled above the first 25mm of weld metal. Welding was stopped at the end of each day but the assembly was maintained at 150 to 205°C for at least 2 hours prior to removing the preheat. Upon completion of the groove the assembly was maintained at 150°-205°C for eight hours prior to removing the preheat. The assembly was not subjected to an intermediate PWHT cycle.

Backing bars and strong backs were removed and the root area ground in preparation for radiographic examination. The complete length of weld was radiographically examined using standard techniques and showed an absence of defects as described by ASME Boiler and Pressure Vessel Code, Section VIII. Repeat examination using high resolution film revealed linear indications over the last 190mm of weld length. These indications were identified as slag inclusions at the root sidewall within the portion of the assembly welded without guidance i.e. within material designated as discard.

Following successful radiographic examination the weld face was locally ground and ultrasonically tested. The complete length of the weld assembly showed an absence of defects and was acceptable to ASME Boiler and Pressure Vessel Code, Section VIII acceptance limits. Magnetic particle examination of both root and face surfaces was performed using the DC yoke method and results were acceptable to ASME Boiler and Pressure Vessel Code, Section VIII.

Table 20 records the results of mechanical tests obtained from the full thickness assembly welded with the Thyssen SlCrMo2 wire and UV 420 TTR flux. Tensile test results show acceptable values compared to the 515 to 690MPa requirements for the base plate specification. Failure of the transverse specimens in the weld metal is a little surprising in view of the expected high strength of narrow groove weld metal and the relatively high values reported (550 to 560MPa) for the base plate. (See Table 7). All sidebend test specimens showed an absence of internal defects.

Weld metal Charpy toughness values at positions required by ASME B & PV Code Section VIII (1.6mm and 1/4t below the plate surface) are in excess of 54J at -40°C, both at the groove 1/2w and 1/4w locations. Contrary to previous test results, toughness values at 1/4w are superior to those at 1/2w. A general deterioration in toughness at the 1/2w location is noted with increasing test depth. At 1/2t and 3/4t the weld metal shows borderline values at -40°C. Toughness values at the 1/4w location remain relatively consistent throughout the depth of the weld.

Base metal Charpy toughness values are consistent through the thickness of plate and compare well with the values in Table 7 provided by the plate manufacturer. Toughness values in the HAZ are all in excess of 54J

at -40°C but only at the 1.6mm and 1/4t depths below the surface do the values exceed those for the corresponding location in the base metal.

The deterioration in weld zone toughness through the depth of the weld may be attributed to self tempering of the weld toward the root or a non-uniform PWHT temperature through the thickness of the weld.

Figure 24 records the results of microhardness surveys at four locations across the weld and no significant difference in hardness is noted from surface to centre thickness.

Chemical analysis performed on samples drilled through the complete thickness is summarized in Table 24. Significant differences are noted between this analysis and those reported during the optimisation experiment (Table 18); Sulphur content is extremely low (0.004 vs. 0.012 percent) and the oxygen content for the 203mm thick weld is approximately half of that previously reported (0.032 vs. 0.068 percent). No explanation is offered for these differences.

9.0 SUMMARY - PRODUCTIVITY DATA

Completion of the full thickness assembly required 92 layers (184 passes) plus 2 capping passes. For a 2.1m long assembly the calculated welding time assuming 100 percent arc efficiency was 11 hours. The actual welding time was recorded at 32 hours for a theoretical 34 percent arc time. Several factors account for the apparent inefficiency.

(a) Only 50 percent of the operator's time is available for welding a longitudinal seam, the balance being used to return the head to the start position, to remove slag after each pass and to recentre the welding head as necessary. During circumferential seam welding, continuous operation occurs because of the self peeling action of the slag during rotation of the vessel.

(b) The narrow preheat temperature range (150 to 205°C) selected from toughness considerations requires periods of inactivity to allow the relatively short assembly to cool below the maximum interpass temperature. This narrow range of preheat temperature would not be a significant problem in production where heat losses occur by radiation and convection.

The calculated wire consumption for the full thickness weldment was 68 kg. The weight of wire consumed during welding this assembly was recorded at 67.6 kg. Flux consumption was 120 kg which implies a 1.8 to 1 flux to wire ratio. This ratio is considered conservative because wastage occurs at the stop and start locations where the flux recovery unit cannot operate in a longitudinal seam.

Table 21 records the measured wire feed speed and calculated deposition rates over the amperage range used during the procedure optimisation experiment. Welding parameters selected for the full thickness assembly are significantly below peak efficiency for a 4mm diameter wire.

In attempt to define more precisely flux consumption, bead on plate welds were made using welding parameters from the optimisation experiment. Flux delivery per unit length was established for each set of parameters prior to welding and flux consumption calculated by difference after welding each bead. The results of this exercise are recorded in Table 22 together with the calculated flux-wire ratios using the deposition rates from Table 21. Flux consumption increases with increase in voltage and decreases with increase in travel speed. These observations are consistent with the effect of primary parameters upon bead shape. For the welding parameters used to weld the full thickness assembly, a practical flux consumption is estimated at 1.5:1 compared to weld wire consumption.

Transverse shrinkage was measured during welding the full thickness assembly using 50mm gauge marks across the face of the weld groove. The shrinkage measured (Table 23) did not occur to the extent (8mm) predicted in Section 7.2.

Negligible angular distortion was measured. The reduced shrinkage for the full thickness assembly may be related to the lower heat input selected to guarantee weld metal toughness but virtual elimination of angular distortion is considered to be of greater significance.

10.0 DISCUSSION

During welding of assemblies in the development program only minor equipment problems were experienced with the ESAB HNG system. This is considered significant for the interrupted useage presented by welding individual test plates since the system is designed primarily for circumferential seams where continuous operation proves the equipment. It is anticipated that during circumferential seam welding no major equipment problems will occur.

The development program has identified flux-wire combinations to attain 54J at-40°C after PWHT from three manufacturers. These consumables are from Thyssen Draht, Oerlikon Industries Inc., and Kawasaki Steel Corporation. Further testing is required to confirm that 54J at -29°C will be met after the Socal step-cooling heat treatment but chemical analysis factors suggest that weld metal produced by any of the three consumables should be acceptable.

The program has also successfully defined the limits to ESO and root gap that the ESAB head will tolerate, welding parameters for capping passes and grinding techniques for in-production weld repairs have been demonstrated.

Two areas require further work. Firstly, weld groove closure on test plates has not been reproducible and predicted joint shrinkage was not seen on the full thickness assembly. Accurate monitoring of the

circumferential seam during Phase III will provide more meaningful distortion data. Secondly, in spite of a large number of assemblies that have been welded and evaluated, the achievement of 54J at -40°C remains unpredictable. Welding parameters that produce acceptable bead appearance and that are economic produce borderline values at 1/4w. Data has shown that less than optimum parameters (450A-34V-61 cm/min travel speed and 204°C interpass temperature) yield acceptable toughness. The superior toughness noted at the groove 1/2w location for 50mm assemblies was not repeated in the full thickness assembly.

The reasons for low toughness appear to be loosely related to macrostructure and weld metal oxygen content but the factors which control -40°C toughness have not been defined. Further development activity is required in order that the macrostructure of 2¼Cr-1Mo weld metal can be accurately characterized. Optical metallography is inadequate to define features of the weld metal structure in the columnar and refined zones. The refined weld metal exhibits at least three zones (coarse grain, fine grain and tempered regions) and the effect of each upon toughness requires clarification.

The degradation of weld zone toughness as test depth increases in the full thickness assembly may be attributed to the tempering effect of successive weld beads and/or a non-uniform PWHT cycle. The exact cause for the toughness distribution noted in the full thickness assembly is unclear again because metallographic features of the 2¼Cr-1Mo weld metal are poorly resolved by optical metallography.

Preliminary productivity data has been compiled from observations made during welding the full thickness assembly and from separate experiments. The welding parameters used to produce acceptable Charpy V-notch toughness are below optimum productivity for a 4mm welding wire although soundness as assessed by radiographic and ultrasonic examinations was completely acceptable.

11.0 REFERENCES

1. De Altama, A. "Submerged Arc Narrow Gap Welding" Metal Construction v12, 10, 1980 pp 520 to 523.

2. Barlow, J.A., "The Effect of Plate Size on the Submerged Arc Weld Thermal Cycle". Welding Institute Research Bulletin, 1982, v23, 3, pp 77-82.

3. Egeman, N. and Nordh, B-A, "Submerged Arc Narrow Gap Welding" Svetsaren, 1, 1982.

4. Baach, H., and Scholz, E. "The Effect of Simulated Heat Treatments on the Mechanical Properties of 2¼Cr-1Mo Type Weld Metals" Schweissmetteilungen, English Edition for Essen Fair v96/97 Sept. 1981, pp 14-19.

5. Anon. "Narrow Gap Submerged Arc Welding Material for 2¼Cr-1Mo Steel - US521N x MF200N". Doc. 0482-147 Welding Division, Kobe Steel.

6. Anon. "Submerged Arc Welded Joint Performance of 305mm Thick 3Cr-1Mo Steel Plate". Kawasaki Steel Corporation.

7. Personal Communication, Dr. H. Dietrich, Thyssen Draht.

8. Metals Handbook, Eighth Edition, v8, Metallography and Phase Diagrams. ASM, Metal Park, Ohio, 1979.

9. Personal Communications, Dr. R. Swift, Luken Steel R&D, Coatesville, Pa.

10. Personal Communications, L. Sarver, Babcock & Wilcox Company, Alliance Research Centre, Alliance, Ohio.

11. ASTM Standards 1982, Part II, Metallography; Nondestructive Testing. E407-Microetching Metals and Alloys. Pub. ASTM, Philadelphia, Pa.

12. Samuels, L.E., "Optical Microscopy of Carbon Steels", Pub. ASM 1980, Metals Park, Ohio.

13. Leggatt, R.H. and White, J.D., "Predicting Shrinkage and Distortion in a Welded Plate" Proc. Conf. Residual Stress in Welded Construction and their Effects", pp 119-132. London, Nov. 1977 Pub. Abington, Cambridge, The Welding Institute 1977.

14. Ohsawa, M. et al, "Distortion of Thick Cylinder Welds by Narrow Groove MIG Welding", IIW Doc. X-1035-83.

15. Davis, O.L., "The Design and Analysis of Industrial Experiments", Pub. Hafhen Publishing Company, Chapter 11, "The Determination of Optimum Conditions".

16. Hill, W.J. and Hunter, W.G., "A Review of Response Surface Methodology: A Literature Survey" Technometrics, v8, 4, Nov. 1966, pp 571 to 590.

TABLE 1: REACTOR VESSEL WELD REQUIREMENTS

FABRICATION & DESIGN CODE:

ASME Boiler and Pressure Vessel Code Section VIII, Div. 1 (Lethal Service).
All pressure retaining welds to be RT, UT and MPE inspected after final PWHT.

MATERIALS:

Shell & Heads:	ASME SA 387, GR22, Cl.2 or SA 335, F22.
Nozzles:	Integrally reinforced main nozzles, ASME SA336, F22
Cladding:	5mm thick stainless steel

MATERIAL REQUIREMENTS:

	Room Temperature	480°C
Tensile Strength, 1/4t:	515-690 MPa	352 MPa min.
Yield Strength, 1/4t:	420 MPa min.	224 MPa min.
Charpy Impact Energy:		
Base Metal, 1/2t:	54J at -40°C after PWHT. 54J TTr -40°C or less after STC.	
Weld Metal, 1/2t:	54J at -40°C after PWHT. 54J TTR -29°C or less after STC.	
Hardness:	225 BHN max. after PWHT	

TABLE 2: PLATE MATERIAL FOR TEST ASSEMBLIES

Chemical Analysis (percent)

Heat No.	Thickness mm	C	Mn	Si	Cr	Mo	S	P	Cu	Ni	Sn	Sb	As	Ti	Cb	V
85155-4	50	0.135	0.56	0.20	2.22	1.00	0.003	0.006	0.07	0.12	0.005	0.002	0.015	0.002	0.011	0.005
13529	9.5	0.13	0.59	0.58	1.35	0.50	0.002	0.017	--	--	--	--	--	--	--	--

Mechanical Properties *

		TS MPa	YS MPa	Percent EL	Percent RA	GS	Cv-40°C	
85155-4	50	585	429	26	77	8	178-201-210	Normalize 925°C, Temper 680°C PWHT 690°C/20h.
							137-154-162	As above plus Socal Step Cool

* Mechanical Properties established at t/2 location.

TABLE 3: WELDING CONSUMABLES FOR FLUX-WIRE EVALUATION

Key	Manufacturer	Description of Wire	Description of Flux	Assembly No.
2.	ESAB AB, (Toronto, Canada)	4mm - OK Autrod V2, Ht. 0946 Cast = 34 cm Helix = 0 cm	OK 10.62, Lot 245876	202
3.	Thyssen Draht AG (Chicago, Illinois)	4mm - Union SlCrMo2 Ht. 537183 Cast = 43 cm Helix = 0 cm	UV 420 TTR, Lot 367508	203
4.	Oerlikon Welding Ind. (Houston, Texas)	4mm - Fluxocord 37 STC, Ht. 032611 Cast = 47 cm Helix = 7.5 cm	OP 76, Lot 081015	204
5.	Union Carbide Ltd. (Toronto, Canada)	5/32 in - Linde U521, Ht. 521002 Cast = 39 cm Helix = 0 cm	Linde 709-5, Lot 0122C3854	205
6.	Kawasaki Steel Corp. (Chiba, Japan)	4mm - KLWT 210, Ht. 36 WOR Cast = 44 cm Helix = 0 cm	KB120, Lot 373152	206
7.	Union Carbide Ltd. (Toronto, Canada)	5/32 in - Linde U521, Ht. 521002 Cast = 39 cm Helix = 0 cm	Linde 124, Lot 0326	207
8.	Kobe Steel Ltd. (Kobe, Japan)	4mm - US 521N, Ht. 8924B Cast = 45 cm Helix = 0 cm	Kobelco MF200N, Lot 3GYA001	208

TABLE 3: (continued)

Key	Description (1)	Basicity Index (1)	Particle Size (1)	Maximum Amperage (1)	Voltage Range (1)	Packaging	Chemical Analysis Percent (2) C	P	S
2	Aggl. Fluoride basic	3.4	--	1000 DC/AC	26-32	Paper bag + plastic liner	0.019	0.06	0.016
3	Aggl. Fluoride basic	2.9	--	800 DC	24-32	Double plastic bag	0.09	0.02	0.004
4	Aggl. Fluoride basic	--	8 x 48	800 DC/AC	--	Steel can + rubber lined lid	0.28	0.02	0.017
5	Fused Neutral	--	12 x 50	800 DC	--	Paper bag + plastic liner	0.02	0.01	0.01
6	Aggl. Fluoride basic	5	120	--	--	Steel can + Al-paper seal at access hole	1.96	0.02	0.012
7	Fused, Fluoride	--	--	--	--	Paper bag	0.03	0.03	0.006
8.	Aggl. Fluoride	--	--	--	--	Steel can + rubber seal at access hole	0.05	0.02	0.007

(1) Data provided by flux manufacturer

(2) Chemical analysis per Galt Testing Laboratories, Cambridge

TABLE 4: RESULTS OF WELDABILITY TESTS

Vendor	Wire Finish	Wire Feed	Flux Feed	Slag Removal	Bead Appearance	Arc Stability	Charpy Toughness	Overall Rating
Linde U521/709-5	3	2	2	2	3	1	4	2.4
Linde U521/124	3	2	3	2	3	1	4	2.6
ESAB	3	2	2	2	2	2	4	2.4
Oerlikon	1	2	2	2	2	1	2	1.7
Thyssen	2	2	2	1	1	3	1	1.7
Kawasaki	1	2	2	2	2	2	2	1.9
Kobe	1	2	3	3	2	2	1	2.0

NOTE:

1 = Good
2 = Average
3 = Poor

and for Charpy Toughness,

1 = greater than 108J
2 = 81 to 108J
3 = 54 to 81J
4 = less than 54J

TABLE 5

EFFECT OF WELDING PARAMETERS UPON MECHANICAL PROPERTIES: P.W.H.T. 20h at 690°C
(Thyssen S1CrMo2 Wire plus UV 420 TTR Flux)

Ass'y No.	A	V	S	T	J	Weld Metal Tensile Properties YS	TS	El %	RA %	Charpy V-Notch Data J, - 40° Weld Metal 1/2t - 1/4w	HAZ 1/2t	Base Metal 1/2t
240	450	26	41	260	17.1	44.5	54.8	32	75	17 24 38 89 154 Avg_3=50 R=137	196 209 236 239 250 Avg_3=228 R=43	--
241	550	30	51	260	19.4	450	552	30	75	16 19 20 27 70 Avg_3=22 R=54	162 166 179 184 238 Avg_3=176 R=76	--
242	650	34	61	260	21.7	453	555	30	75	21 21 62 74 111 Avg_3=53 R=90	158 171 176 206 233 Avg_3=184 R=75	--
243	450	26	41	177	17.1	456	554	30	76	15 25 35 35 99 Avg_3=32 R=84	106 152 202 225 233 Avg_3=192 R=127	--
244	650	34	61	177	21.7	447	549	29	74	24 30 62 69 69 Avg_3=51 R=45	192 230 240 250 261 Avg_3=240 R=69	132 134 146 150 154 Avg_3=143 R=22
222	450	26	61	11.5	20.4					15-21 21 29 47 Avg_3=23 R=32		
223	450	26	61	11.5	31.6					9 13 15 15 15 Avg_3=14 R=6		
224	450	34	61	15.0	20.4					83 102 109 112 118 Avg_3=108 R=35		
ASME SA387 Gr22 C12 Acceptance Criteria						310 min.	515 to 690	18 min.	45 min.	54 min.	54 min.	54 min.
ASME SFA-5.23 F84-EB3-B3 Acceptance Criteria						410 min.	550 to 690	20 min.	--	27 min.	27 min.	27 min.

TABLE 6

MATRIX OF WELDING PARAMETERS FOR PROCEDURE OPTIMISATION

Assembly No.	Travel Speed, S cm/min.	Amperage	Voltage	Interpass Temp. °C
212	51	550	30	260*
213	41	450	26	204
214	41	450	26	316
215	41	450	34	204
216	41	450	34	316
217	41	650	26	204
218	41	650	26	316
219	41	650	34	204
220	41	650	34	316
221	51	550	30	260*
222	61	450	26	204
223	61	450	26	316
224	61	450	34	204
225	61	450	34	316
226	61	650	26	204
227	61	650	26	316
228	61	650	34	204
229	61	650	34	316
230	51	550	30	260*

* Reference

TABLE 7

PLATE MATERIAL FOR FULL THICKNESS ASSEMBLY

Supplier:	C-L Marrel, Rive-de-Gier, France
Material:	ASME SA387 Gr22 Cl.2 1980 Edition
Heat No.:	85155
Condition:	Austenitise 7h 50m at 925°C Water Quench Temper 6h 20m at 680°C, Air Cool
Test Coupons:	As above plus 20h PWHT at 690°C with heating and cooling rates above 427°C of 56°C/h. plus Socal Step Cool Cycle

Chemical Analysis: (percent)

C	Mn	Si	S	P	Ni	Cr	Mo	Cu	Sn	Sb	As	Ti	Cb	V
0.13	0.56	0.20	0.003	0.006	0.12	2.21	1.02	0.07	0.005	0.002	0.014	0.002	0.002	0.005

Mechanical Properties: Transverse Test at 1/4t, Room Temperature

	TS MPa	TS MPa	El Percent	RA Percent	G.S.	Cv-40°C, J PWHT	Cv-40°C, J STC
Top	409	563	30	77	8	221	163
Bottom	395	552	31	79	00	285	242

TABLE 8: CHEMICAL ANALYSIS OF FILLER WIRE (wt. percent) (1)

KEY	C	Mn	Si	Cr	Mo	S	P	Cu	Ni	Sn	Sb	As	Ti	Cb	V	Al(5)
2	0.13	0.460	0.210	2.545	1.01	0.005	0.0053	0.150	0.065	0.0043	0.0033	0.0031	0.005	0.01	0.005	0.007
3	0.100	0.430	0.135	2.64	1.05	0.007	0.0064	0.065	0.040	0.006	0.0008	0.0027	0.005	0.01	0.005	0.002
4 (2)	0.12	0.755	0.180	2.59	1.10	0.007	--	0.085	0.050	--	--	--	0.005	0.01	0.015	--
5	0.125	0.585	0.120	2.475	1.01	0.008	0.011	0.095	0.140	0.0020	0.0030	0.0047	0.005	0.01	0.005	0.021
6	0.115	0.535	0.085	2.29	1.02	0.006	0.0057	0.260	0.030	0.0012	0.0021	0.0012	0.005	0.01	0.015	0.002
8	0.130	0.605	0.180	2.55	1.06	0.004	0.0064	0.100	0.155	0.0010	0.0024	0.0025	0.005	0.01	0.005	0.10

(1) Chemical Analysis performed by EMR. Elements Cr-Mo-Mn-Ni-Cu-Ti-Cb-V by Spectrographic Analysis. C and S by combustion. Balance by Wet Chemical Analysis.

(2) Filler wire No. 3 is a flux cored product; chemical analysis is taken from weld deposit prepared in accordance with AWS 5.23.

TABLE 9: CHEMICAL ANALYSIS OF WELD DEPOSIT (wt. percent) (1)

Ass'y	C	Mn	Si	Cr	Mo	S	P	Cu	Ni	Sn	Sb	As	Ti	Cb	V	Al(2)	O(3)	N(3)	J(4)	X(5)
202	0.070	0.585	0.260	2.42	0.885	0.008	0.012	0.160	0.060	0.0050	0.0036	0.0040	0.005	0.01	0.005	0.014	0.039	0.012	144	16
203	0.073	0.657	0.210	2.47	0.995	0.008	0.007	0.055	0.030	0.0020	0.0031	0.0037	0.005	0.01	0.005	0.009	0.038	0.016	78	10
204	0.095	0.755	0.160	2.49	1.060	0.010	0.015	0.072	0.042	0.0053	0.0033	0.0036	0.005	0.01	0.015	0.007	0.022	0.010	186	19
205	0.059	0.695	0.315	2.27	0.940	0.010	0.013	0.105	0.140	0.0024	0.0039	0.0056	0.005	0.01	0.005	0.002	0.061	0.016	155	16
206	0.120	0.840	0.205	2.12	0.972	0.008	0.007	0.230	0.020	0.0016	0.0038	0.0020	0.005	0.01	0.080	0.002	0.050	0.004	79	10
207	0.060	0.690	0.400	2.22	0.975	0.010	0.013	0.100	0.140	0.0024	0.0030	0.0054	0.005	0.01	0.005	0.005	0.077	0.016	168	16
208	0.100	0.530	0.342	2.34	0.985	0.008	0.008	0.095	0.155	0.0015	0.0043	0.0031	0.005	0.01	0.005	0.020	0.047	0.031	83	11

(1) Chemical analysis performed by EMR. Elements Cr-Mo-Mn-Ni-Cu-Ti-Cb-V by spectrographic analysis. C and S by combustion. Balance by Wet Chemical Analysis.

(2) Total aluminum

(3) O and N analysis performed by National Spectrographic Labs, Cleveland, Ohio.

(4) $J = (Mn + Si).(P + Sn) \times 10^4$

(5) $X = \frac{10P + 5Sb + 4Sn + As}{100}$ (ppm)

TABLE 10

COMPARISONS OF WELD DEPOSIT TO WELD WIRE ANALYSIS

Percent Change in Elemental Analysis Referred to Wire Analysis

Assembly No.	C	Mn	Si	Cr	Mo	Ni	As	Al
202	-46	+27	+23	-9	-12	-8	+20	+100
203	-27	+53	+55	-6	-5	-25	+37	+350
205	-57	+19	+162	-8	-7	0	+19	-90
206	+4	+57	+141	-7	-5	-33	+67	0
207	-52	+18	+233	-10	-3	0	+15	-76
208	-23	-12	+90	-8	-7	0	+24	-80

TABLE 11: CHARPY V-NOTCH TEST RESULTS

Assembly No.	Impact Energy (J)	Lateral Expansion (mm)	% Shear
202 (ESAB)	14	0.356	10
	16	0.279	10
	20	0.330	10
	61	0.813	15
	79 Avg. 32	1.092	15
203 (Thyssen)	27	0.584	30
	81	1.041	35
	130	1.778	55
	137	1.880	55
	155 Avg. 116	1.981	55
204 (Oerlikon)	87	1.219	40
	92	1.372	60
	92	1.546	60
	104	1.473	65
	122 Avg. 96	1.702	65
205 (Linde 709-5)	23	0.457	10
	27	0.457	20
	41	0.584	15
	46	1.711	30
	57 Avg. 38	0.864	25
206 (Kawasaki)	85	1.219	45
	87	1.168	45
	87	1.194	45
	92	1.270	65
	92 Avg. 89	1.295	65
207 (Linde 124)	14	0.229	5
	16	0.330	5
	31	0.483	10
	34	0.584	10
	38 Avg. 27	0.533	10
208 (Kobe)	100	1.422	80
	80	1.549	80
	108	1.473	80
	114	1.346	80
	114 Avg. 110	1.702	80

TABLE 12

EFFECTS OF NOTCH LOCATION ON WELD METAL TOUGHNESS (-40°C)

Assembly 203 (Thyssen)			Assembly 208 (Kobe)			Assembly 204 (Oerlikon)		
Impact Energy J	Lat. Expan. mm	Percent Shear	Impact Energy J	Lat. Expan. mm	Percent Shear	Impact Energy J	Lat. Expan. mm	Percent Shear
Initial Results of 1/4t x 1/2w								
27	0.584	30	80	1.422	80	87	1.219	40
81	1.041	35	100	1.473	80	92	1.372	60
130	1.778	55	108	1.702	80	92	1.546	60
137	1.880	55	114	1.346	80	104	1.473	65
155	1.981	55	114	1.702	80	122	1.702	65
Ave (3) = 116			Ave (3) = 103			Ave (3) = 96		
Ave (5) = 106			Ave (5) = 107			Ave (5) = 99		
Range = 128			Range = 34			Range = 35		
Non-Refined Zone (1/4t x 1/4w)								
17	0.254	21	75	1.245	50	8		
35	0.559	31	77	1.143	42	18	0.483	5
53	0.762	27	83	1.270	61	19	0.254	0
65	0.940	33	87	1.397	53	34	0.508	10
128	1.956	52	94	1.600	59	42	0.660	10
Ave (3) = 51			Ave (3) = 84			Ave (3) = 24		
Ave (5) = 59			Ave (5) = 82			Ave (5) = 24		
Range = 111			Range = 19			Range = 34		
Centre Refined Zone (1/2t x 1/2w)								
30	0.432	26	94	1.549	70	Not Tested		
84	1.219	40	100	1.448	80			
112	1.549	50	103	1.524	70			
114	1.651	50	123	1.626	77			
179	2.413	67	125	1.575	79			
Ave (3) = 103			Ave (3) = 109					
Ave (5) = 104			Ave (5) = 109					
Range = 149			Range = 31					

TABLE 13

ETCHING REAGENTS USED TO DEVELOP MACROSTRUCTURE

OF 2 1/4 Cr-1Mo WELDS AFTER 10h PWHT AT 690°C

ETCHANT	DESCRIPTION	REFERENCE
1.	Nital - 10ml/HNO_3 and 90 ml Alcohol	8
2.	Vilella's Reagent - 5ml HCl + 1gm Picric Acid + 100ml Alcohol	8
3.	5-10% Acetic Acid 5-20% HNO_3 H_2O	9
4.	2% Iodine in Alcohol	10
5.	50ml. HCl/50 ml H_2O (70-82°C)	8
6.	Fry's Reagent 40 ml HCl - 5g $CuCl_2$ - 30 ml H_2O - 25ml Alcohol	11
7.	50 ml H_2SO_4/40 ml H_2O	11
8.	10 ml HNO_3 - 40 ml HCl - 30ml Glycerol	11
9.	1 part HNO_3 1 part Acetic Acid	12
10.	45g $CuCl_2$ - 180 ml HCl - 100 ml H_2O	8
11.	5g $FeCl_3$ - 10 ml HCl - 10 ml HNO_3 - 5 ml H_2SO_4 - 75 ml H_2O	8

TABLE 14

DIMENSIONAL ANALYSIS OF NARROW GROOVE WELDS

Assembly Number	Bead Depth (*) mm	Average Depth of Non-Refined Weld mm (Range)	Average Depth of Refined Weld mm (Range)	Ratio of Non-Refined To Refined Structure
202	8.15	2.8 (2.15 to 4.05)	0.50 (0.40 to 0.65)	5.5
203	7.9	2.5 (1.90 to 3.15)	0.75 (0.40 to 1.00)	3.3
204	5.8	2.8 (2.05 to 3.55)	0.40 (0.25 to 1.15)	7.1
205	7.9	2.5 (1.50 to 3.15)	0.90 (0.75 to 1.50)	2.9
206	7.6	2.7 (1.25 to 3.30)	0.90 (0.50 to 1.00)	3.0
207	7.6	2.0 (0.90 to 3.15)	1.00 (0.75 to 1.40)	2.0
208	7.6	2.8 (2.30 to 4.45)	0.65 (0.50 to 1.00)	4.3

* Measured at top bead location

TABLE 15: SHRINKAGE DATA FOR 50mm TEST ASSEMBLIES

Assembly No.	Shrinkage Across Groove Face (mm)		Shrinkage Across Groove Root (mm)		Approx. Lateral Distortion (mm)
202	3.2	3.2	na	na	na
203	1.9	1.7	na	na	na
204	1.9	1.95	0.51	0.64	na
205	2.3	1.85	1.00	0.64	0.89
206	3.6	3.4	0.86	0.94	1.27
207	1.8	1.2	0.71	na	2.03
208	3.2	3.2	0.66	0.79	2.03
Average	2.57	2.21	0.75	0.75	1.55

TABLE 16

DIMENSIONAL ANALYSIS OF NARROW GROOVE WELDS - VARIABLE ESO

Assembly Number	Bead Depth (*) mm	Average Depth of Non-Refined Weld mm	Average Depth of Refined Weld mm	Average Side Wall Penetration mm
232 (ESO = 40mm)	7.95	1.30 (0.75 - 1.88)	1.95 (1.36 - 2.55)	1.50 (0.74 - 1.58)
233 (ESO = 48mm)	8.05	1.00 (0.56 - 1.40)	1.85 (1.47 - 2.38)	1.30 (0.70 - 1.26)
234 (ESO = 54mm)	8.40	1.20 (1.26 - 1.60)	1.65 (1.30 - 2.12)	1.40 (0.70 - 2.52)

* Measured at Top Bead Location

TABLE 17

RESULTS FROM OPTIMISATION EXPERIMENTS
(All Assemblies were welded with Thyssen SlCrMo2 Wire and UV 420 TTR flux)

Ass'y No.	A	V	S	J	T	W	Dg	DNG	Cg	Fg	Pg	F C+F	H	Va	Peak Hardness HAZ	WM	Cv
212	550	30	512	19.4	260	16	9	10.5	1.8	1.8	0.7	50	3	100	410	360	
221	550	30	51	19.4	260	16	8.5	10	1.9	1.7	0.8	47	2.5	0	365	350	
230	550	30	51	19.4	260	15	8	9.5	1.7	1.9	0.6	53	2.5	0	350	355	
241	550	30	51	19.4	260				1.4	2.4		64					22
215	450	34	41	22.4	204	15.5	9.1	8.5	1.8	1.3	0.7	42	3	0	330	330	
216	450	34	41	22.4	316	14.5	7.5	6	2.0	1.6	1.3	44	3.5	0	350	350	
243	450	26	41	17.1	177				2.0	1.4		41					32
213	450	26	41	17.1	204	14	6	6.5	1.8	1.6	0.6	47	2	0	380	360	
240	450	26	41	17.1	260				0	All		100					50
214	450	26	41	17.1	316	15	4.5	5	0	All	0.7	100	3	0	280	335	
222	450	26	61	11.5	204	12.5	6	6	0	All	0.4	100	1.5	0	375	360	23
223	450	26	61	11.5	316	12.5	6.5	5	0	All	0.4	100	2	0	390	350	14
224	450	34	61	15.0	204	11	6.5	6.5	0	All	0.8	100	2.5	0	385	365	108
225	450	34	61	15.0	316	13.5	8	7.5	0	All	0.8	100	3	0	340	355	
226	650	26	61	16.6	204	12.5	11	12.5	3.1	1.0	0.3	24	2	0	320	360	
227	650	26	61	16.6	316	12.5	12	11.5	2.8	1.4	0.3	33	2.5	0	350	350	
244	650	34	61	21.7	177				2.7	2.0		43					51
228	650	34	61	21.7	204	14	11	12	1.2	2.0	0.9	37	3	0	390	365	
242	650	34	61	21.7	260				3.1	2.0		39					53
229	650	34	61	21.7	316	15	12	11	1.8	1.8	0.8	50	3	0	360	335	
217	650	26	41	24.7	204	14	13.5	13.5	4.5	1.6	0.3	26	3	50	390	350	
218	650	26	41	24.7	316	14	13.5	13.5	3.4	1.9	0.9	36	3	100	365	350	
219	650	34	41	32.3	204	17.5	13.5	13.5	3.4	1.9	0.9	36	3	100	365	350	
220	650	34	41	32.3	314	17	14	13	3.0	@.0	1.4	40	4	100	380	360	

W = Bead Width mm
D = Bead Depth mm
g = Guided Wall
ng = Non-Guided Wall

C = Coarse Grain mm
F = Fin Grain mm
P = Penetration mm
Va = Ferrite Veining

U = Undercut
Po = Porosity
H = HAZ Width mm
Cv = Charpy V-Notch Toughness -40°C, J.

S = Travel Speed cm/min
J = Heat Input KJ/cm
T = Interpass Temp. °C

TABLE 18

EFFECT OF CHEMICAL ANALYSIS ON TOUGHNESS

Ass'y No.	Welding Parameters A - V - S - J - IT	Analysis (Percent) C	Mn	Si	Cr	Mo	S	P	Cu	O	N	Cv-40° J
212	550 - 30 - 41 - 19.4 - 260	0.09	0.53	0.20	2.60	0.99	0.014	0.015	0.04	0.062	0.015	--
241	550 - 30 - 51 - 19.4 - 260	0.09	0.56	0.22	2.48	1.00	0.011	0.014	0.03	0.058	0.014	22
240	450 - 26 - 41 - 17.1 - 260	0.07	0.53	0.21	2.54	1.03	0.015	0.015	0.03	0.061	0.014	50
243	450 - 26 - 41 - 17.1 - 177	0.08	0.55	0.19	2.49	0.99	0.013	0.014	0.03	0.056	0.014	32
222	450 - 26 - 61 - 11.5 - 204	0.08	0.50	0.21	2.59	1.00	0.012	0.013	0.04	0.081	0.014	23
223	450 - 26 - 61 - 11.5 - 316	0.06	0.54	0.22	2.59	1.02	0.012	0.012	0.03	0.091	0.013	14
224	450 - 34 - 61 - 15.0 - 204	0.07	0.56	0.20	2.50	1.05	0.013	0.014	0.04	0.068	0.013	108
242	660 - 34 - 61 - 21.7 - 260	0.06	0.54	0.20	2.53	0.98	0.012	01014	0.02	0.058	0.014	53
244	650 - 34 - 61 - 21.7 - 177	0.09	0.54	0.21	2.50	1.00	0.014	0.011	0.03	0.056	0.014	51
218	650 - 26 - 41 - 24.7 - 316	0.08	0.47	0.20	2.60	0.99	0.012	0.011	0.04	0.068	0.013	--

TABLE 19

WELDING PARAMETERS FOR FULL THICKNESS ASSEMBLY

	Groove Weld	Capping Pass
Preheat Temperature	150°C minimum	190°C minimum
Interpass Temperature	205°C maximum	205°C maximum
Amperage	450 ± 25	550 ± 25
Voltage	34 ± 1	34 ± 1
Travel Speed	61 cm/min	51 cm/min
Electrical Stick Out	46mm	46mm
Wire to Wall Distance	2.4mm	--

4mm dia. wire - Thyssen SlCrMo2 Heat 437183

Flux - Thyssen UV 420 TTR Lot 367508

TABLE 20

MECHANICAL PROPERTIES FOR FULL THICKNESS ASSEMBLY (PWHT 20h at 650°C)

Welding Consumables: Thyssen SlCrMo2 wire (Heat 437183) and
Thyssen UV 420 TTR Lot 367508

a. Mechanical Properties (Room Temperature)

Reduced Section Tensile Test (ASME B & PV Code, Section IX, Fig. QW 462.1(a))

	TS MPa	Type and Location of Fracture
1a	578	Ductile in weld metal
1b	572	Ductile in weld metal
2a	598	Ductile in weld metal
2b	594	Ductile in weld metal

b. Side Bend Tests [ASME B & PV Code, Section IX, Fig. QW 462.2(a)]

Side bends free of open defects.

TABLE 20 (continued)

WELD METAL TOUGHNESS

Location	Cv-40°C, J	Lateral Expansion, mm	Percent Shear
1.6mm - 1/2w	50 - 56 - 98 - 104 - 129 Avg. = 86	0.84 - 0.97 - 1.42 - 1.47 - 1.80	10 - 20 - 30 - 35 - 35
1.5mm - 1/4w	96 - 126 - 130 - 146 - 168 Avg. = 135	1.47 - 2.00 - 2.06 - 2.31 - 2.44	20 - 25 - 30 - 30 - 35
1/4t - 1/2w	76 - 106 - 121 - 122 - 123 Avg. = 117	1.14 - 1.58 - 1.73 - 1.85 - 1.80	15 - 25 - 35 - 30 - 25
1/4t - 1/4w	103 - 123 - 126 - 127 - 130 Avg. = 127	1.58 - 1.91 - 1.83 - 1.83 - 1.80	20 - 20 - 25 - 30 - 30
1/2t - 1/2w	23 - 24 - 47 - 76 - 88 Avg. = 49	0.48 - 0.48 - 0.94 - 1.17 - 1.30	10 - 10 - 20 - 20 - 25
1/2t - 1/4w	64 - 108 - 123 - 136 - 138 Avg. = 122	1.52 - 1.55 - 1.63 - 1.91 - 2.31	20 - 30 - 40 - 35 - 35
	Cv-29°C, J		
3/4t - 1/2w	28 - 42 - 57 - 96 - 121 Avg. = 65	0.64 - 0.74 - 1.19 - 1.42 - 1.60	10 - 10 - 15 - 25 - 25
3/4t - 1/4w	140 - 149 - 150 - 169 - 171 Avg. = 157	2.03 - 2.03 - 2.03 - 2.18 - 21.3	40 - 45 - 50 - 45 - 65

TABLE 20 (continued)

BASE METAL CHARPY TOUGHNESS

Location	Cv-40°C, J	Lateral Expansion, mm	Percent Shear
1.6mm	192 - 194 - 201 - 271 - 278 Avg. = 223	2.29 - 2.41 - 2.31 - 2.52 - 2.57	45 - 45 - 45 - 50 - 45
1/4t	176 - 180 - 194 - 228 - 281 Avg. = 201	2.49 - 2.52 - 2.52 - 2.49 - 2.46	50 - 50 - 50 - 45 - 40
1/2t	156 - 168 - 179 - 260 - 267 Avg. = 203	2.36 - 2.31 - 2.69 - 2.41 - 2.44	40 - 45 - 50 - 45 - 40
	Cv-29°C, J		
3/4t	192 - 254 - 260 - 271 - 275 Avg. = 263	2.44 - 2.62 - 2.46 - 2.62 - 2.29	40 - 45 - 45 - 45 - 35

HAZ CHARPY TOUGHNESS

	Cv-40°C, J		
1.6mm	183 - 244 - 256 - 259 - 267 Avg. = 255	2.39 - 2.52 - 2.31 - 2.16 - 2.06	75 - 75 - 70 - 65 - 65
1/4t	163 - 186 - 239 - 241 - 248 Avg. = 223	2.24 - 2.06 - 2.64 - 2.13 - 2.39	50 - 45 - 40 - 40 - 40
1/2t	136 - 136 - 175 - 217 - 226 Avg. = 177	1.78 - 1.93 - 2.36 - 2.03 - 2.41	45 - 40 - - 45 - 50
	Cv-29°C, J		
3/4t	165 - 167 - 176 - 182 - 258 Avg. = 176	1.75 - 2.34 - 2.13 - 2.26 - 2.31	35 - 40 - 40 - 45 - 35

TABLE 21

CALCULATED DEPOSITION RATE WITH WELDING CURRENT

(4mm Dia. Thyssen S1CrMo2 + UV 420 TTR)

Amps.	Volts	WFS cm/mm	Deposition Rate kgm/hr.
450	26	91	5.37
450	34	94	5.58
550	30	122	7.20
650	26	183	10.8
650	34	152	8.98

TABLE 22

FLUX CONSUMPTION DATA

(4mm Dia. Thyssen SlCrMo2 Wire plus UV 420 TTR Flux)

A	V	S	Flux Consumed gm/cm	Slag Produced gm/cm	Weld Deposit gm/cm	Flux Wire Ratio
450	26	41	31.5	1.45	2.18	1.44:1
450	34	41	3.50	2.20	2.27	1.54:1
450	26	61	1.50	1.00	1.47	1.02:1
450	34	61	2.00	1.45	1.52	1.31:1
550	30	51	2.65	1.45	2.35	1.13:1
650	26	41	2.75	1.85	4.39	0.65:1
650	34	41	4.65	2.40	3.65	1.27:1
650	26	61	1.40	1.00	2.95	0.48:1
650	34	61	2.50	1.60	2.45	1.02:1

TABLE 23

TRANSVERSE SHRINKAGE FOR FULL THICKNESS ASSEMBLY

Distance from Weld Start cm	Transverse Shrinkage * mm
15	3.94
45	3.83
76	3.76
106	3.86
137	3.83
168	3.76
198	3.53

* Measured at 149°C after completion of weld groove.

TABLE 24

WELD METAL ANALYSIS OF FULL THICKNESS ASSEMBLY (Percent)(1)

C	Mn	Si	Cr	Mo	S	P	Cn	O	N
0.072	0.067	0.024	2.30	1.03	0.004	0.011	0.05	0.032	0.014

(1) Analysis by National Spectrographic Laboratories.

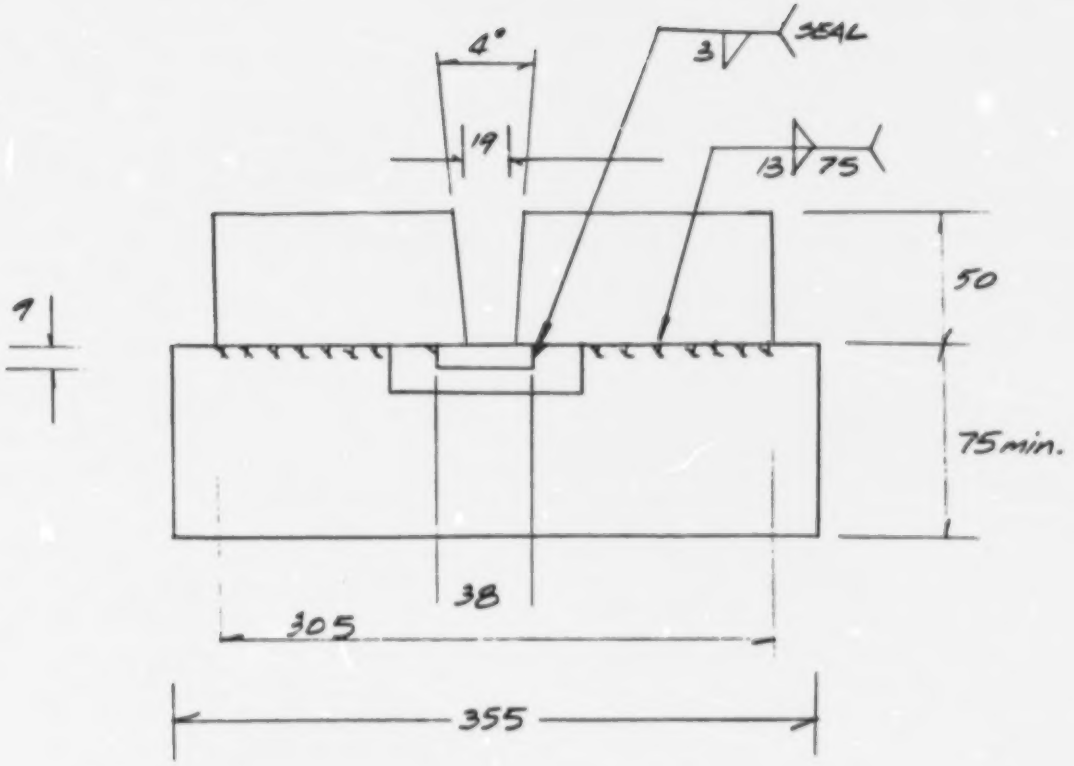

FIGURE 1: Test Assembly Design
Test assembly consists of two 2¼Cr-1Mo plates, one 9mm thick x 38mm wide 1¼Cr-½Mo backing bar and three equidistant strong backs 50mm thick x 75mm high x 355 mm wide

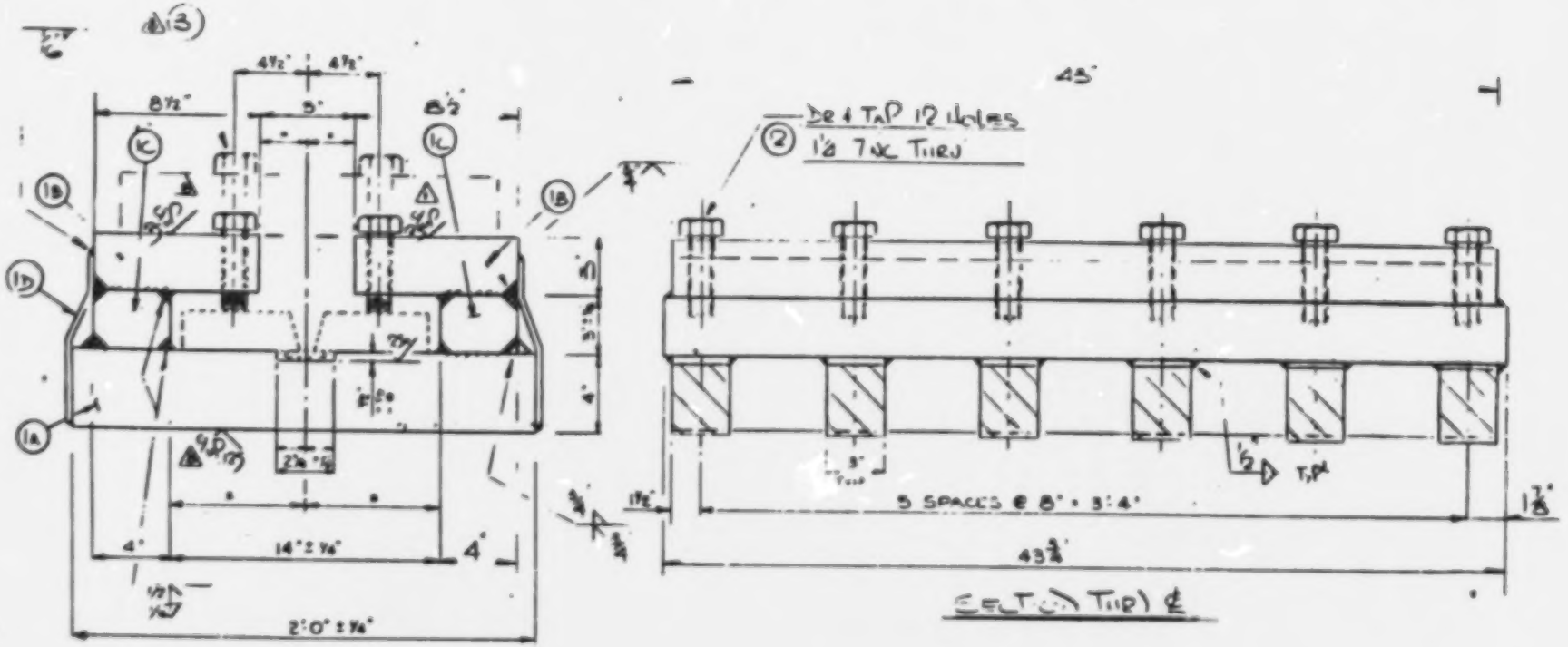

FIGURE 2: Test Plate Hold Down Fixture Design

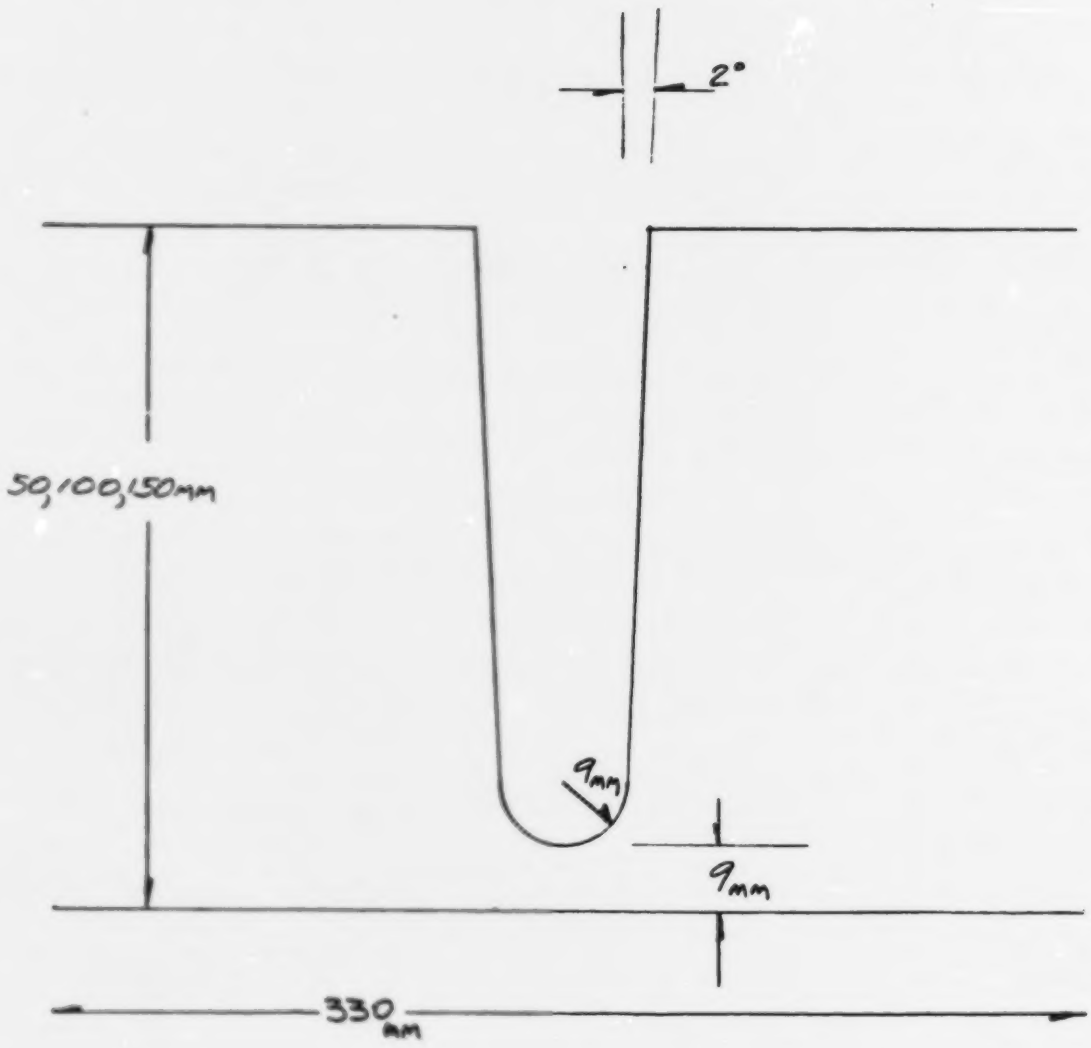

FIGURE 3: Test Plate Design for Shrinkage Determination

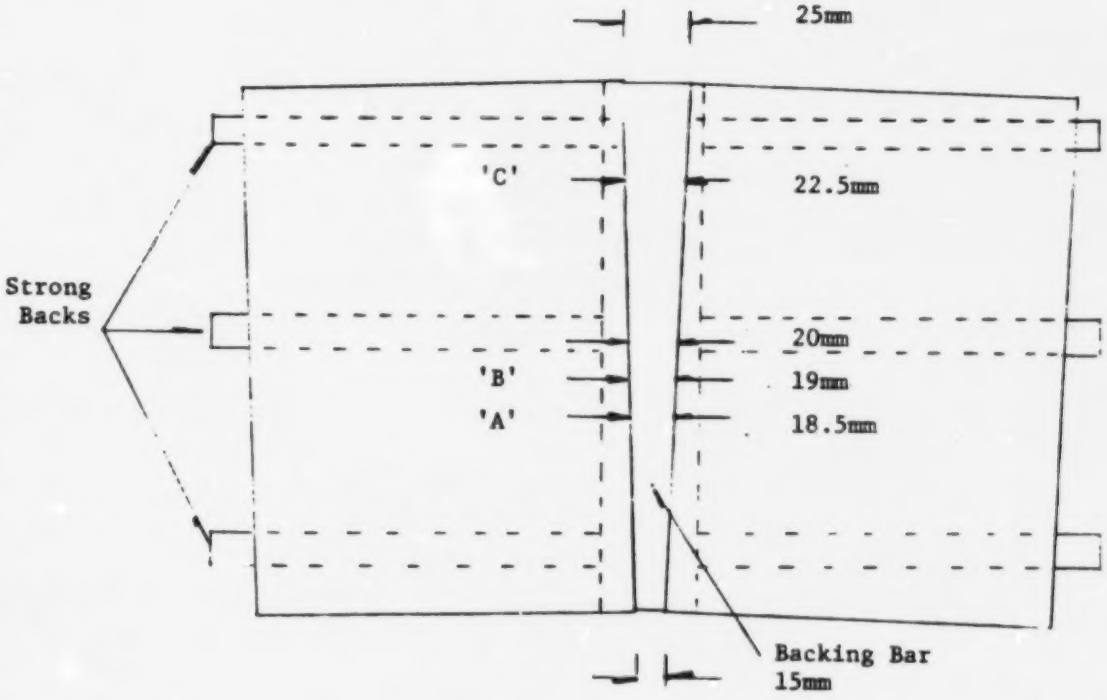

FIGURE 4: Test Assembly for Root Gap Evaluation

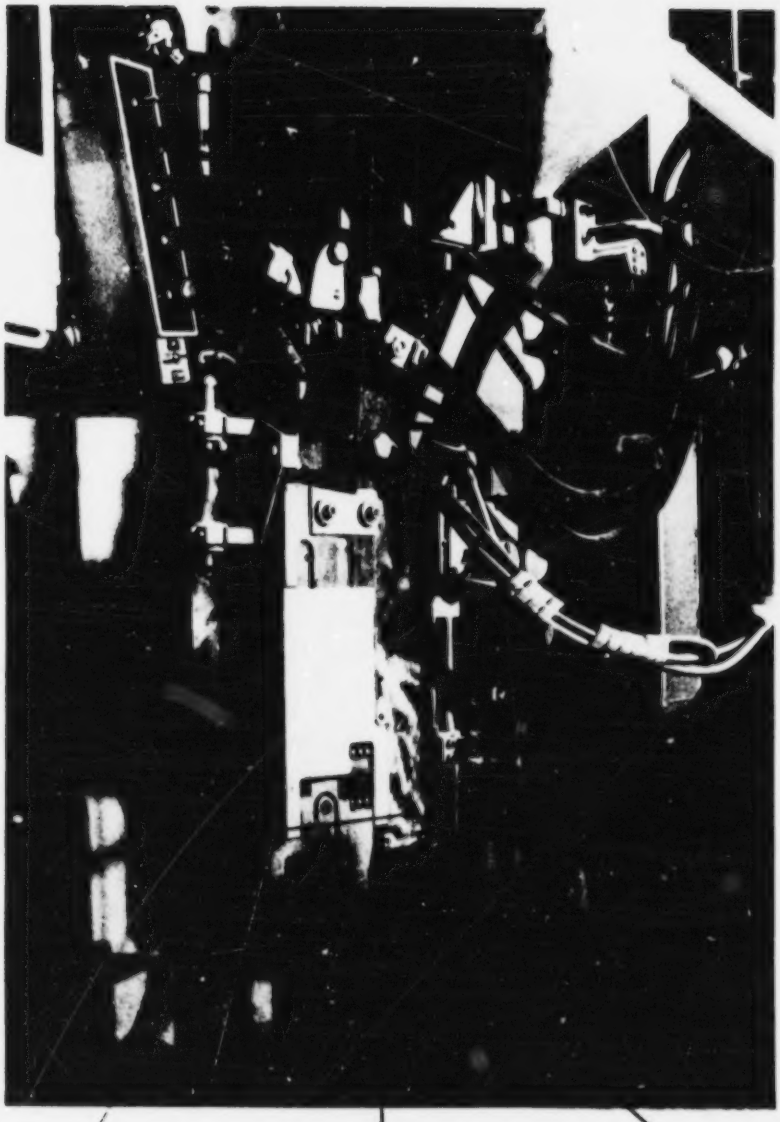

FIGURE 5: Detail of the Esab Welding Head

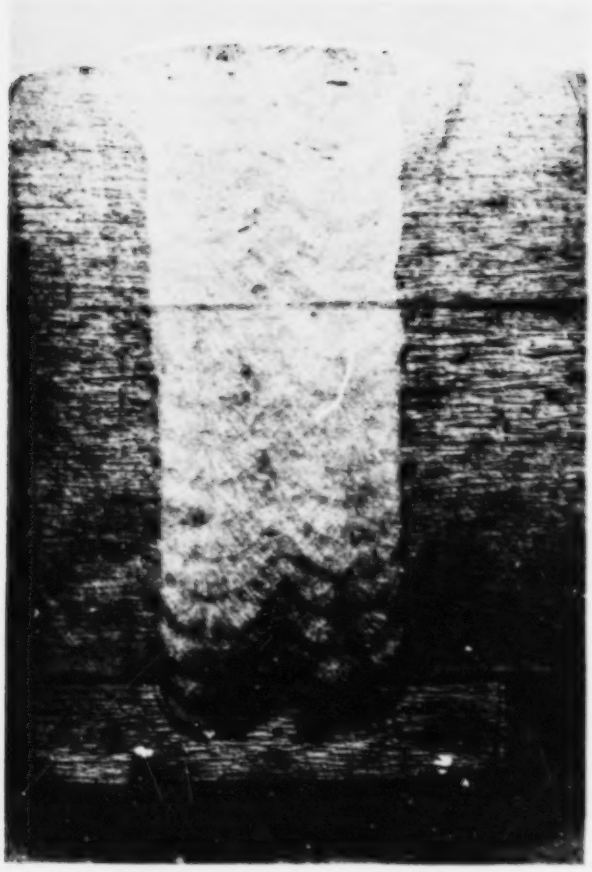

FIGURE 6: Cross Section of Narrow Groove Weld
Etched: Ammonium Persulphate
Magnification x 1.5

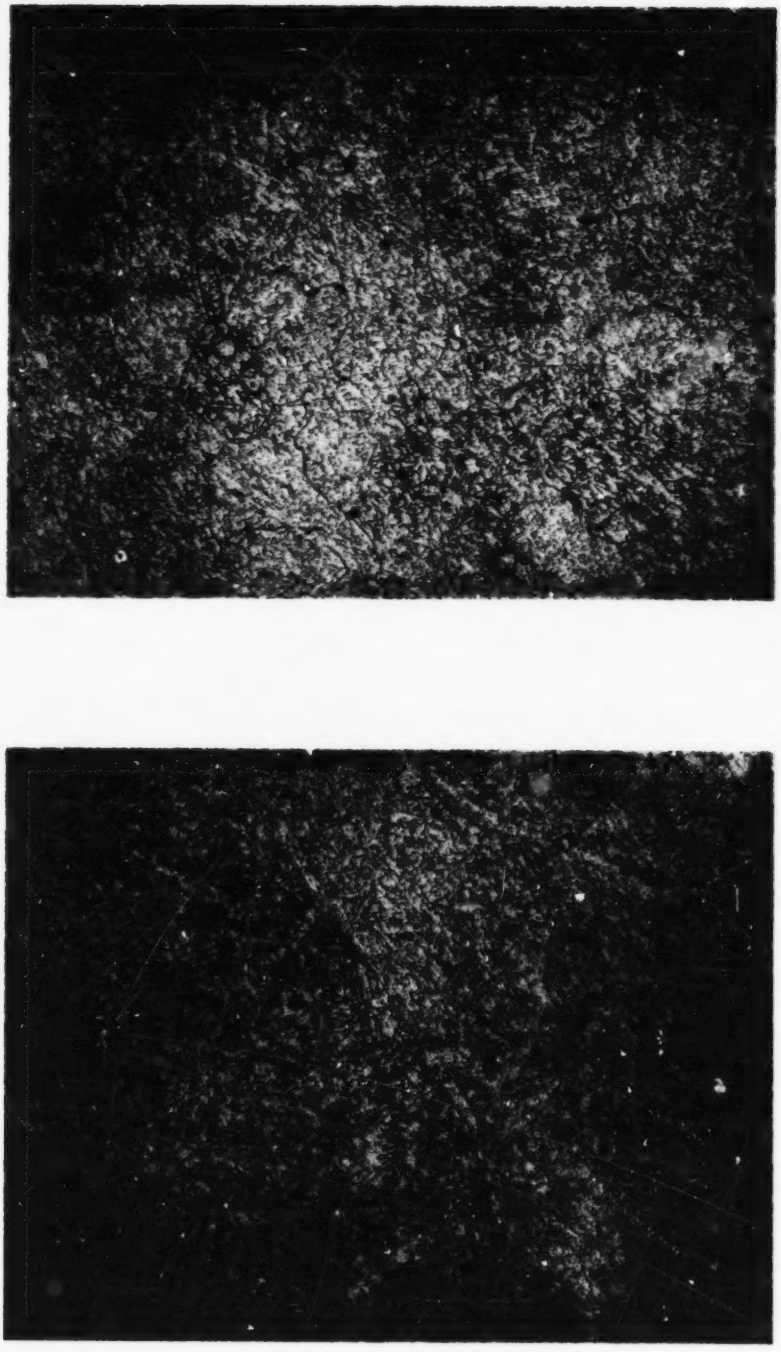

FIGURE 7: Microstructure of Weld 202
Tempered Bainite in Columnar Region (bottom) and
Refined Zone (top) of 2¼Cr-1Mo Narrow Groove Weld

Etched 2% Nital. Magnification x 200

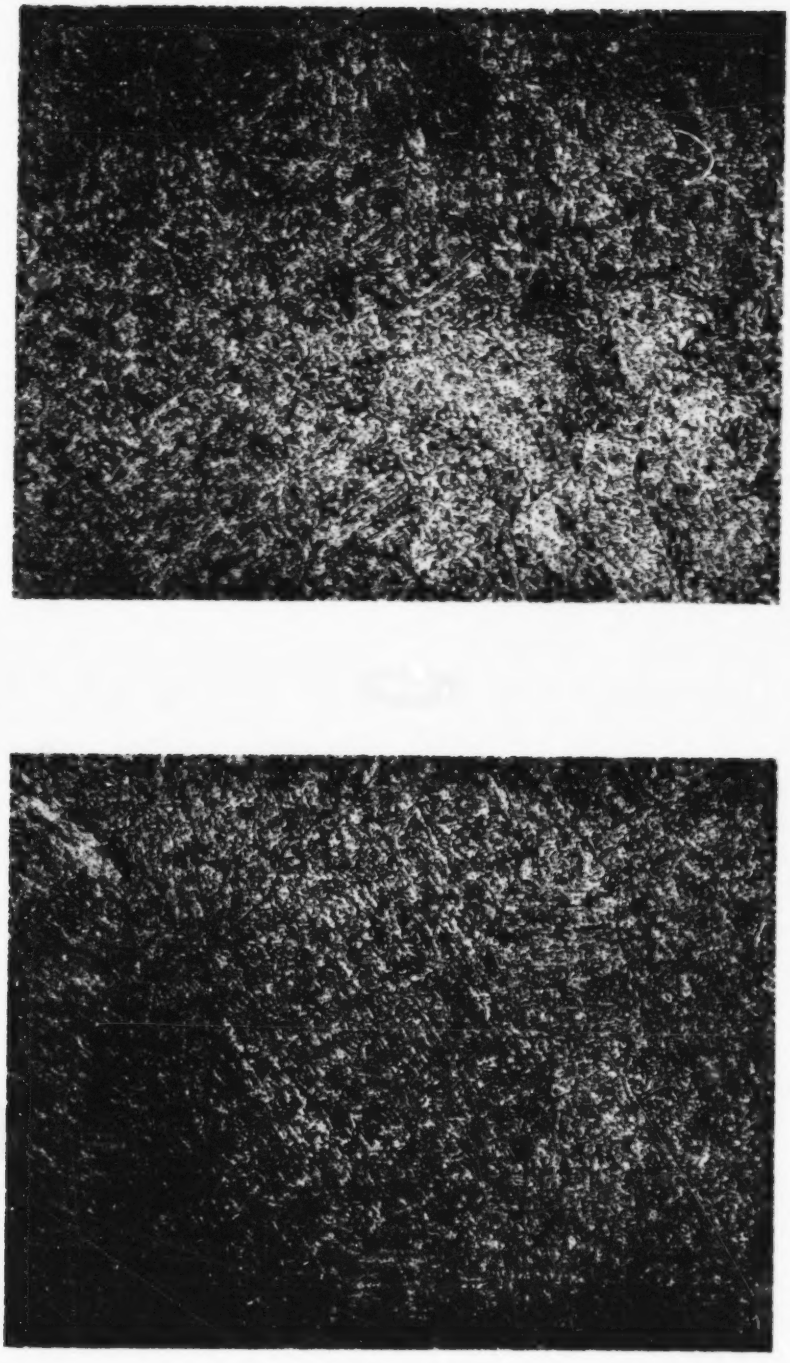

FIGURE 8: Microstructure of Weld 203
Tempered Bainite in Columnar Region (bottom) and
Refined Zone (top) of 2¼Cr-1Mo Narrow Groove Weld

Etched 2% Nital. Magnification x 200

FIGURE 9: Microstructure of Weld 204
Tempered Bainite in Columnar Region (bottom) and
Refined Zone (top) of 2¼Cr-1Mo Narrow Groove Weld

Etched 2% Nital. Magnification x 200

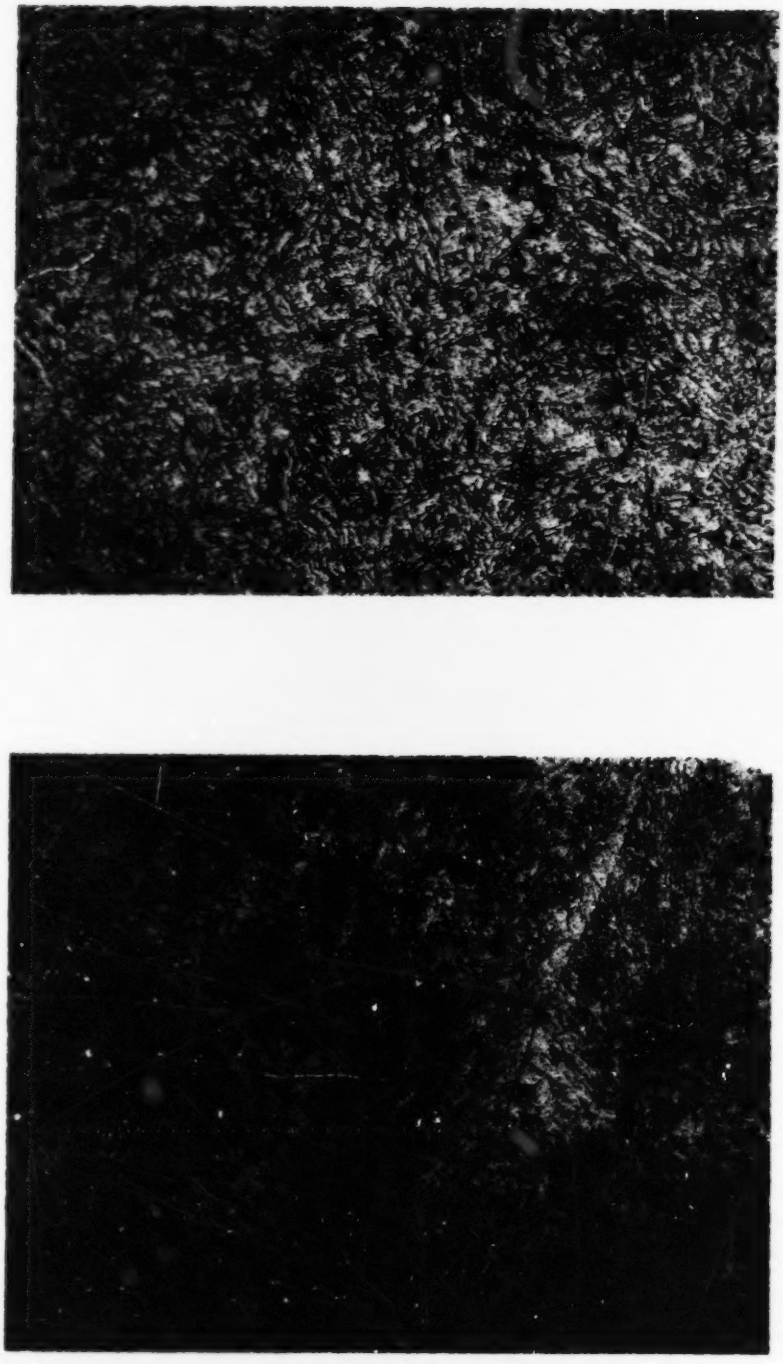

FIGURE 10: Microstructure of Weld 205
Tempered Bainite in Columnar Region (bottom) and
Refined Zone (top) of 2¼Cr-1Mo Narrow Groove Weld

Etched 2% Nital. Magnification x 200

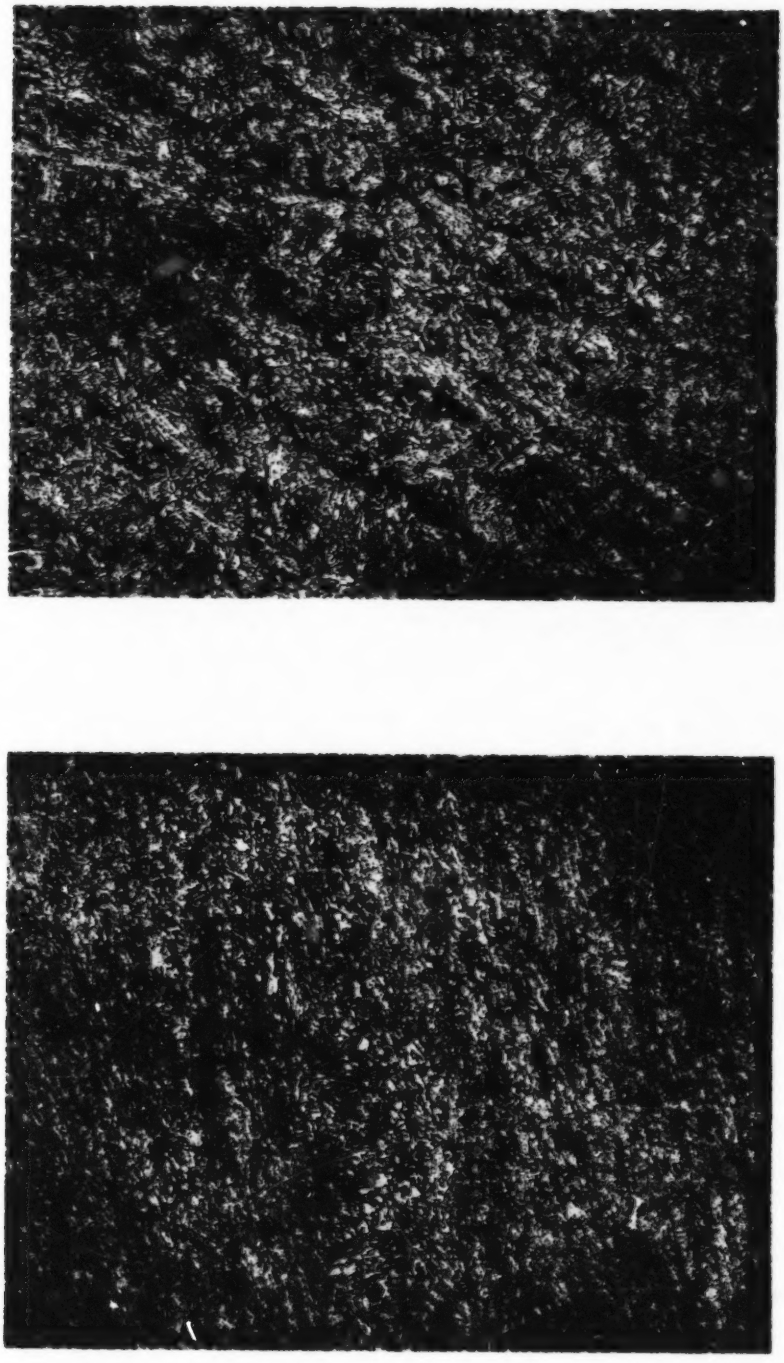

FIGURE 11: Microstructure of Weld 206
Tempered Bainite in Columnar Region (bottom) and
Refined Zone (top) of 2¼Cr-1Mo Narrow Groove Weld

Etched 2% Nital. Magnification x 200

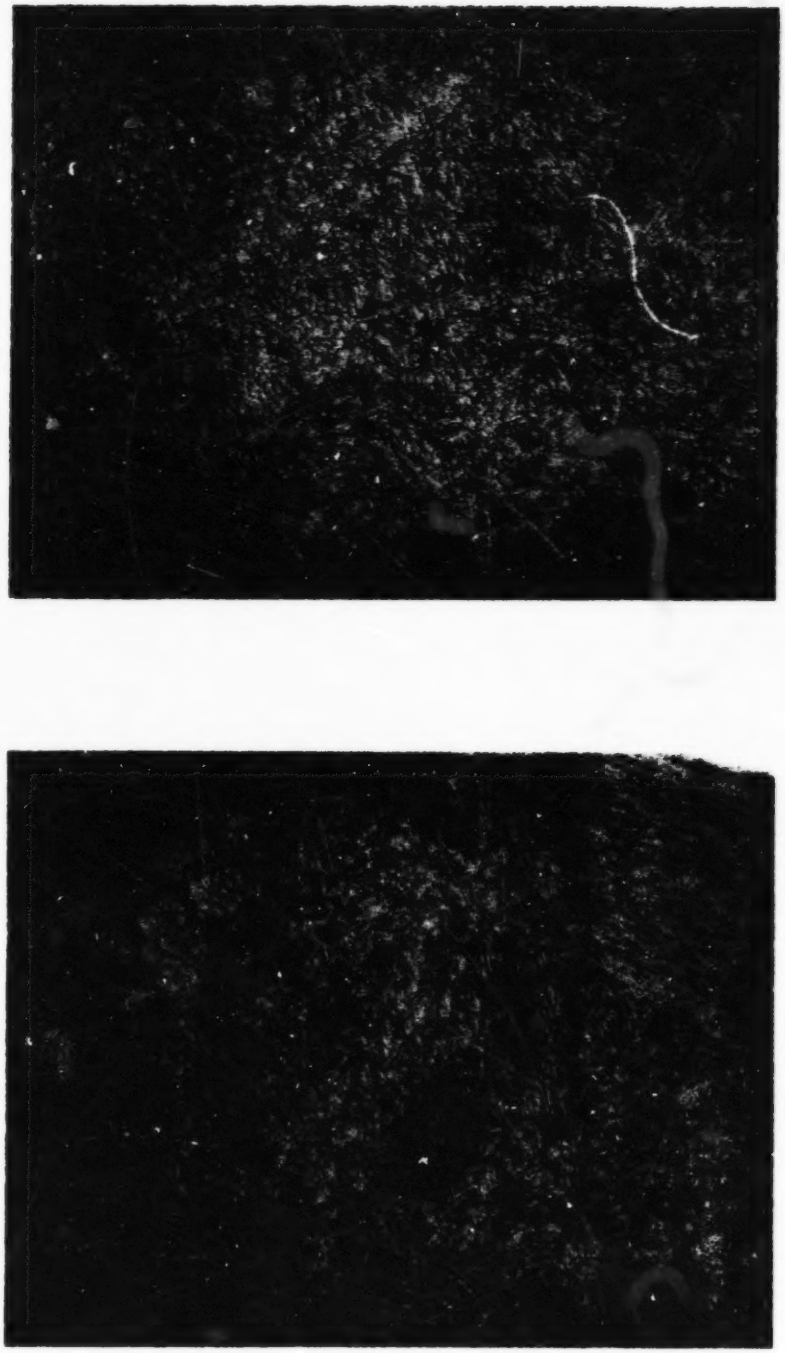

FIGURE 12: Microstructure of Weld 207
Tempered Bainite in Columnar Region (bottom) and
Refined Zone (top) of 2¼Cr-1Mo Narrow Groove Weld

Etched 2% Nital. Magnification x 200

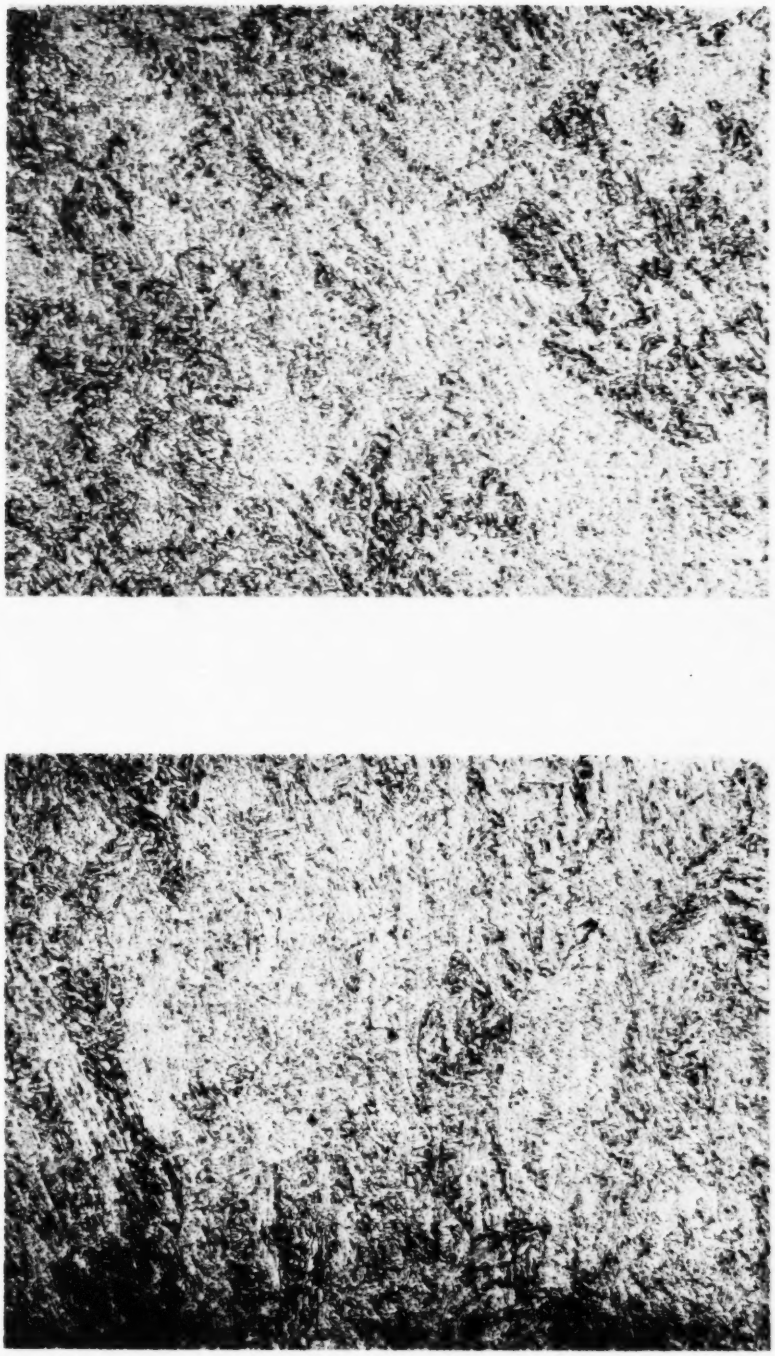

FIGURE 13: Microstructure of Weld 208
Tempered Bainite in Columnar Region (bottom) and
Refined Zone (top) of 2¼Cr-1Mo Narrow Groove Weld

Etched 2% Nital. Magnification x 200

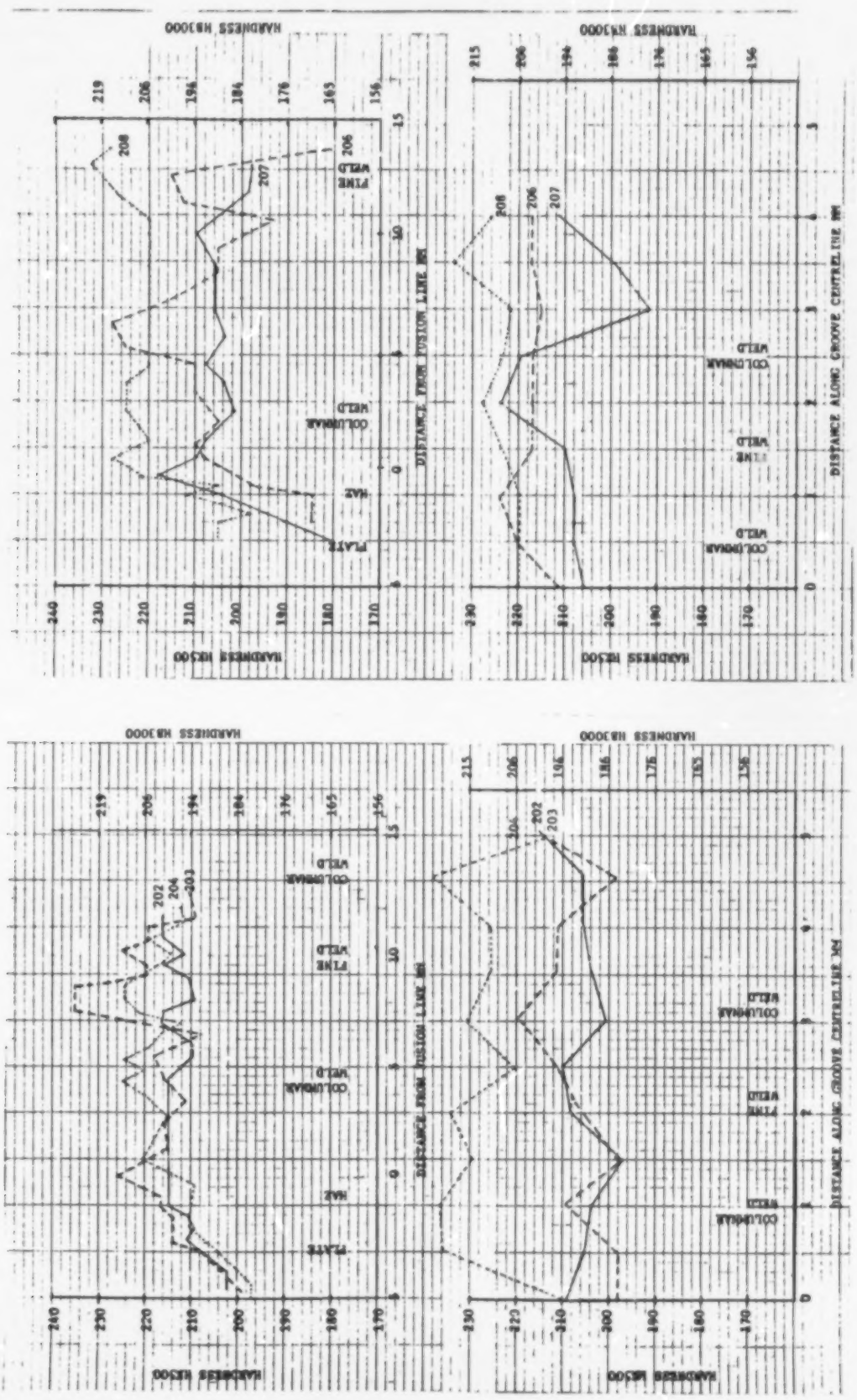

FIGURE 14: MICRO HARDNESS SURVEY THROUGH NARROW GROOVE WELDMENTS

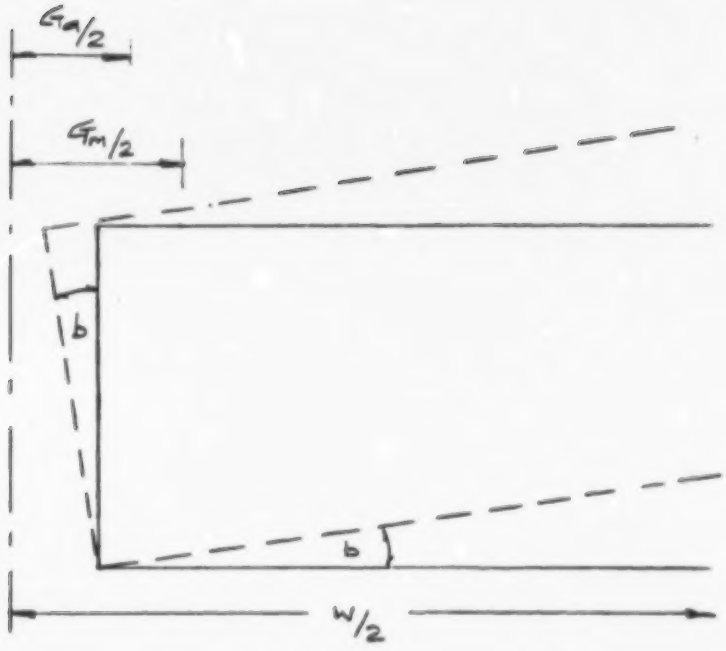

FIGURE 15: Representation of Groove Wall Shrinkage and Distortion

G_m = Groove Shrinkage

G_a = Groove Shrinkage Resulting From Angular Distortion

b = Angular Distortion

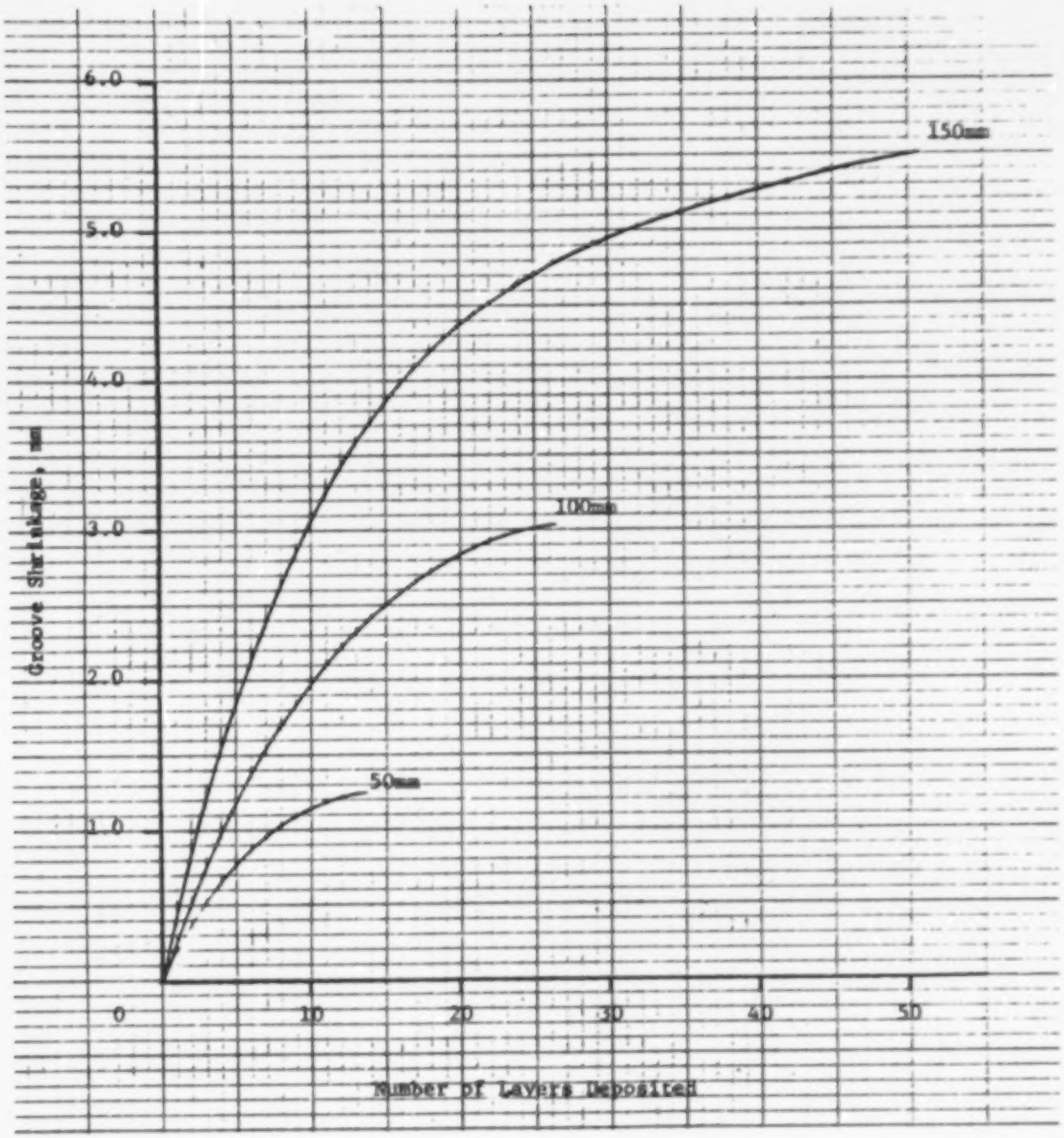

FIGURE 16: Relation of Groove Shrinkage to Depth of Weld

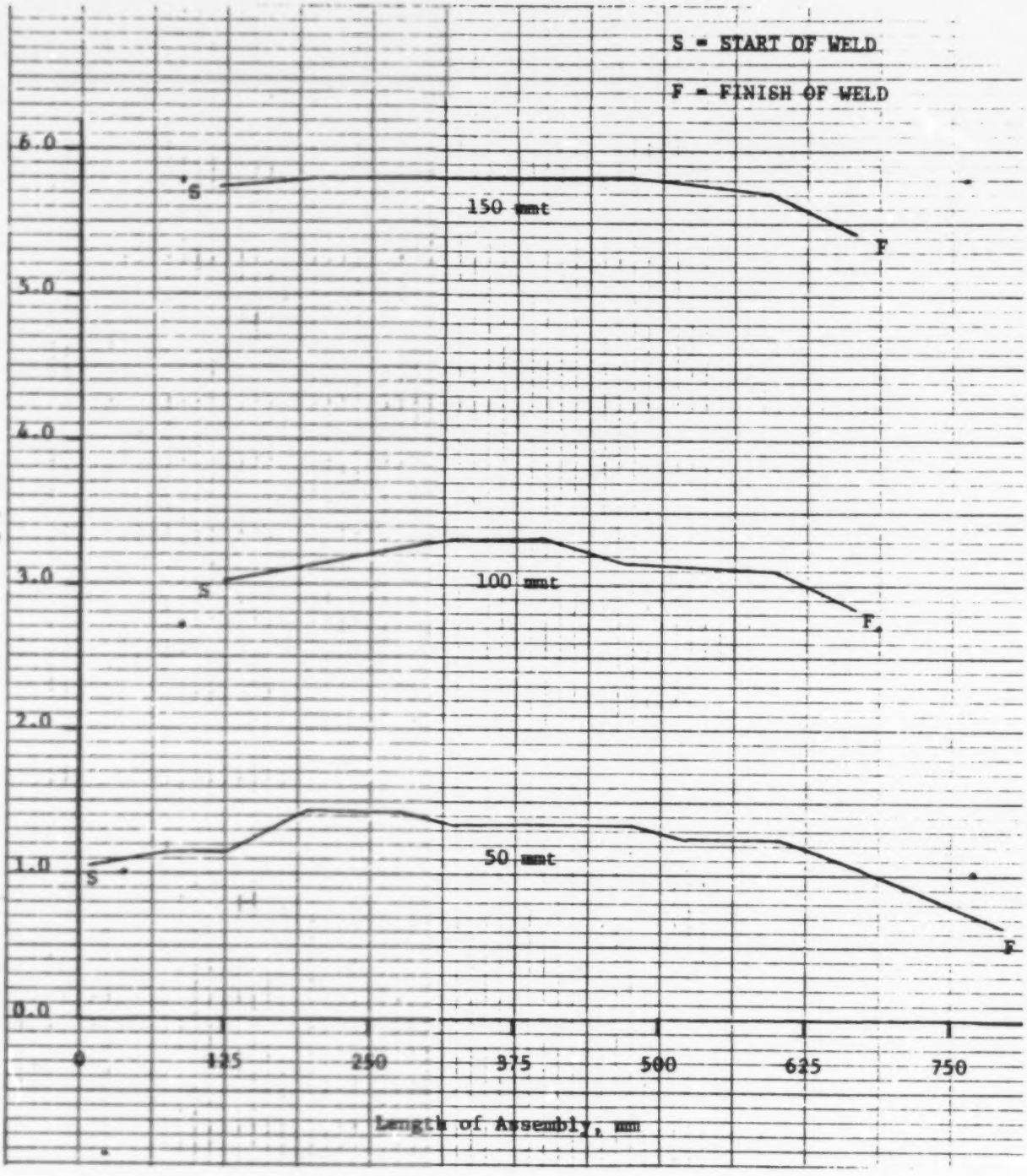

FIGURE 17: Distribution of Groove Shrinkage with Weld Length

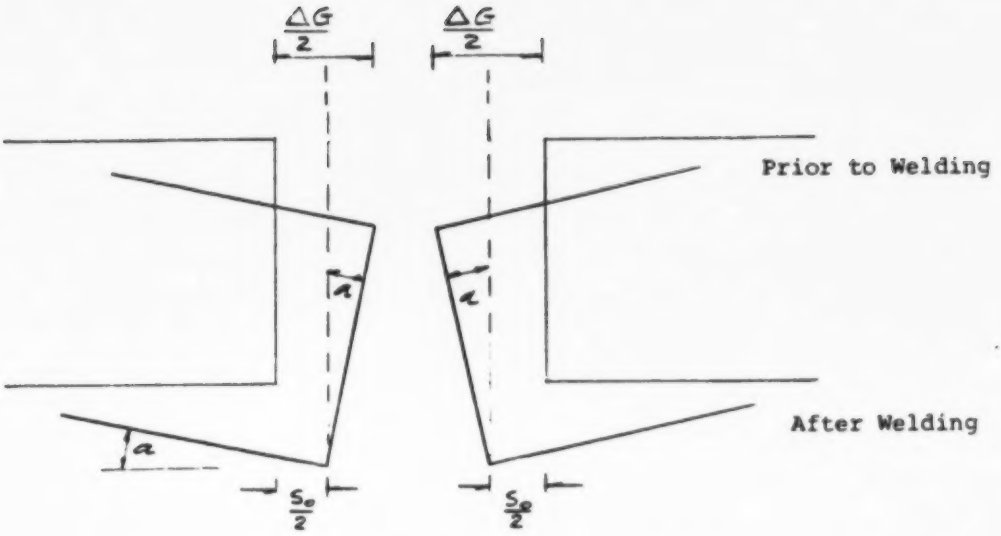

FIGURE 18: Representation of Groove Distortion (14)

G = Groove Shrinkage

S_o = Root Shrinkage

a = Angular Distortion

For 50mm plate, $a = \tan^{-1}\left(\frac{1.5}{2} \times \frac{1}{50.8}\right) = 0.85°$

For 100mm plate, $a = \tan^{-1}\left(\frac{3.5}{2} \times \frac{1}{101.6}\right) = 0.99°$

For 150mm plate, $a = \tan^{-1}\left(\frac{5.8}{2} \times \frac{1}{152.4}\right) = 1.09°$

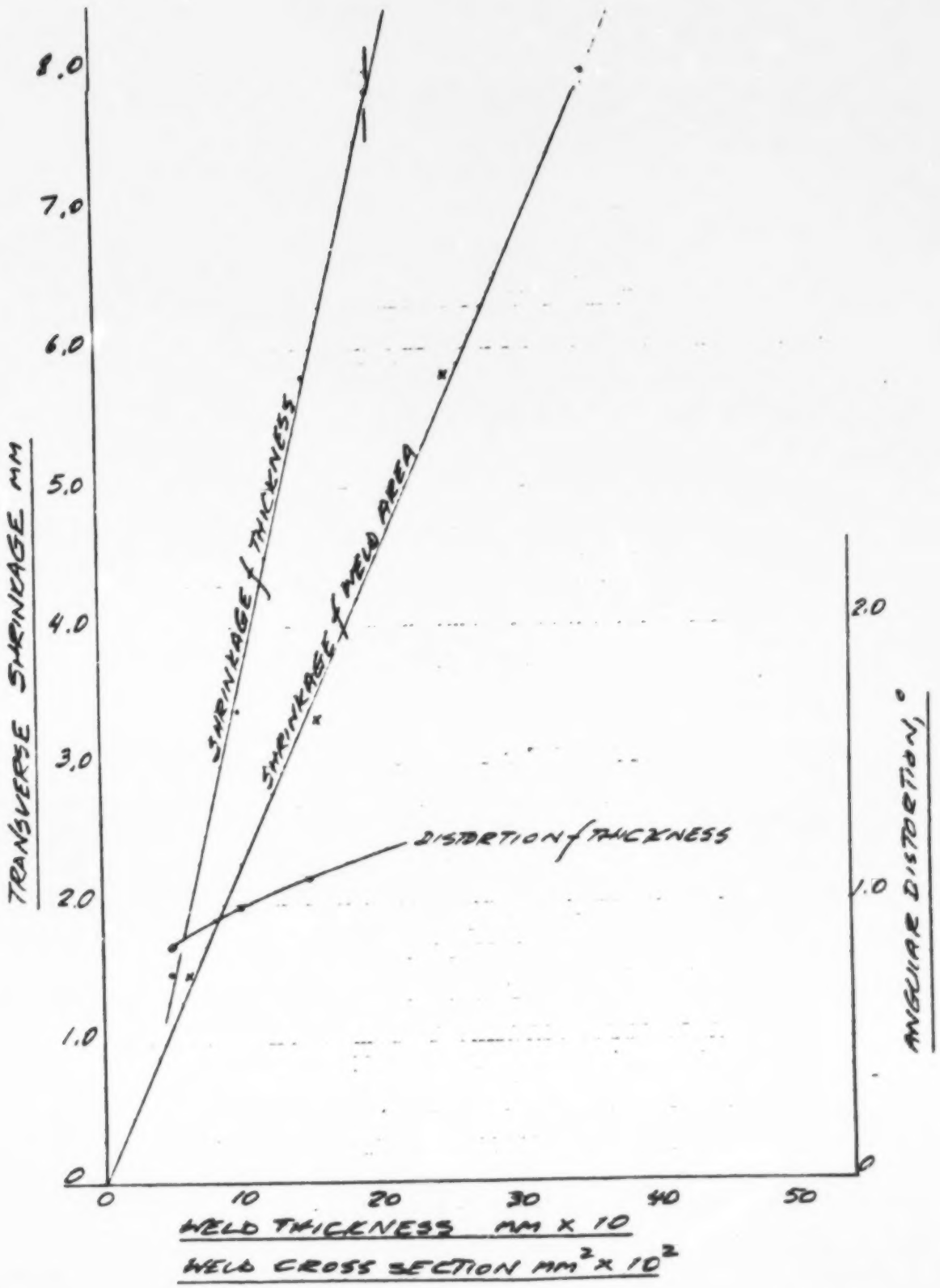

FIGURE 19: Relation of Transverse Shrinkage with Weld Size

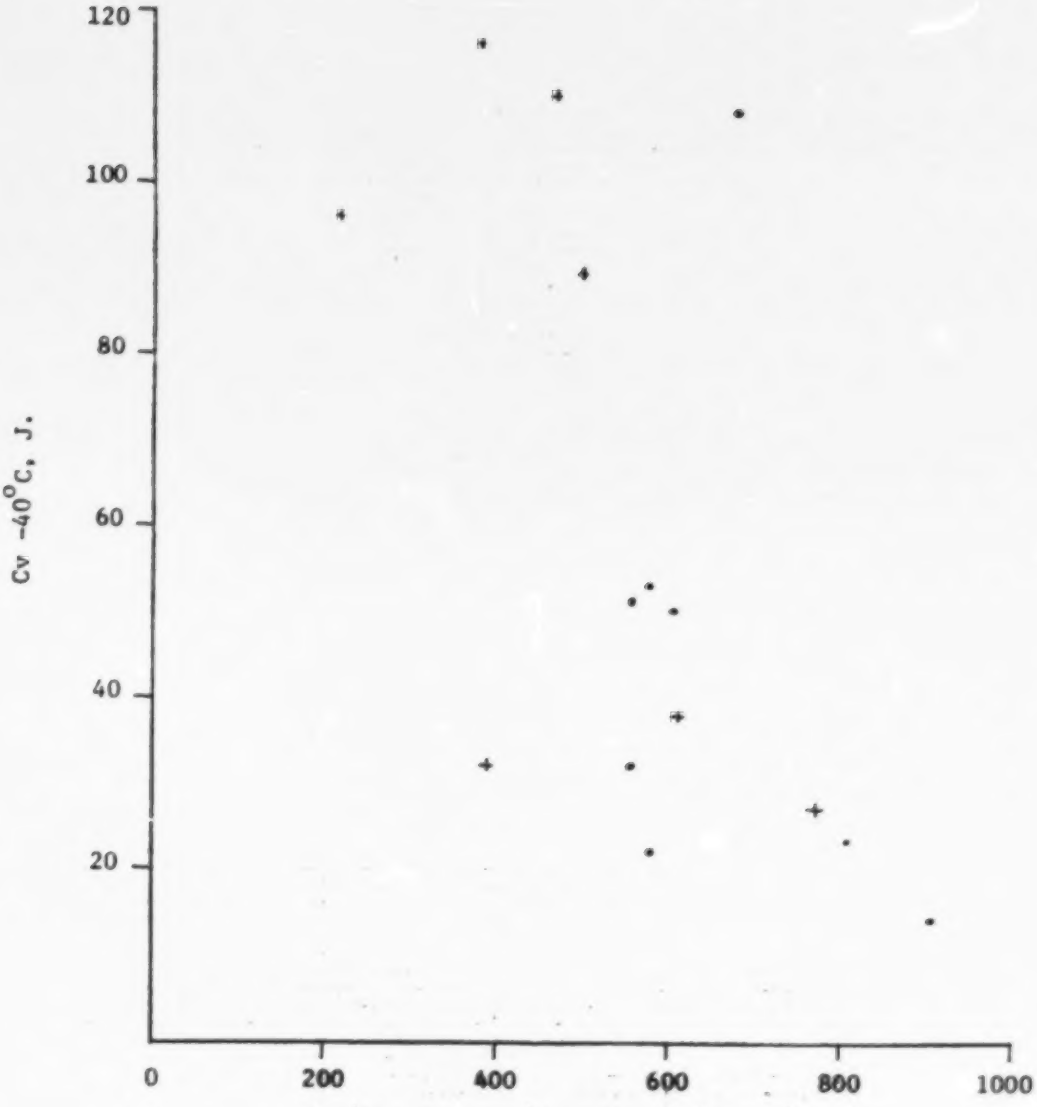

Data plotted from Tables 5, 9, 11, 12 and 18.

FIGURE 20: Effect of Weld Metal Oxygen upon Toughness

. 1/4w ± 1/2w

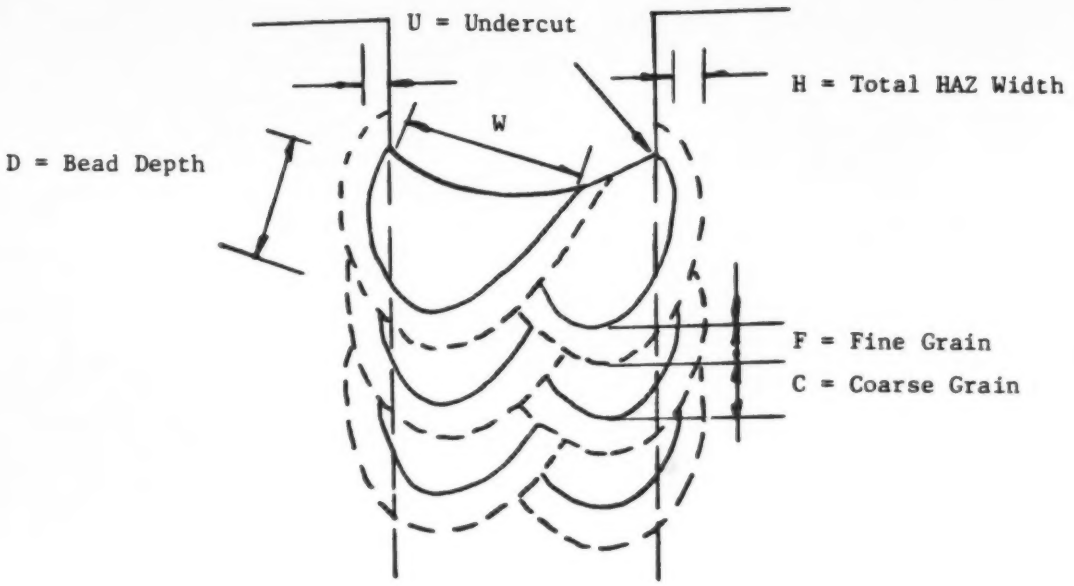

FIGURE 21: Summary of Weld Dimensional Examination

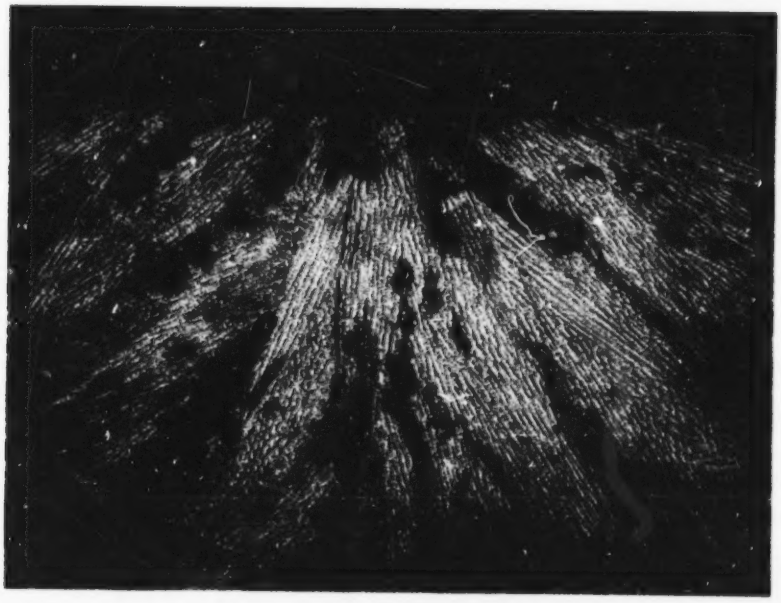

FIGURE 22: Ferrite Veining in the Last Bead of Assembly 232
Magnification x 20 top, x 50 bottom

Etchant: Ammonium Persulphate

FIGURE 23: Cross Section Through Full Thickness Weld
(Reduced approx. 0.75)

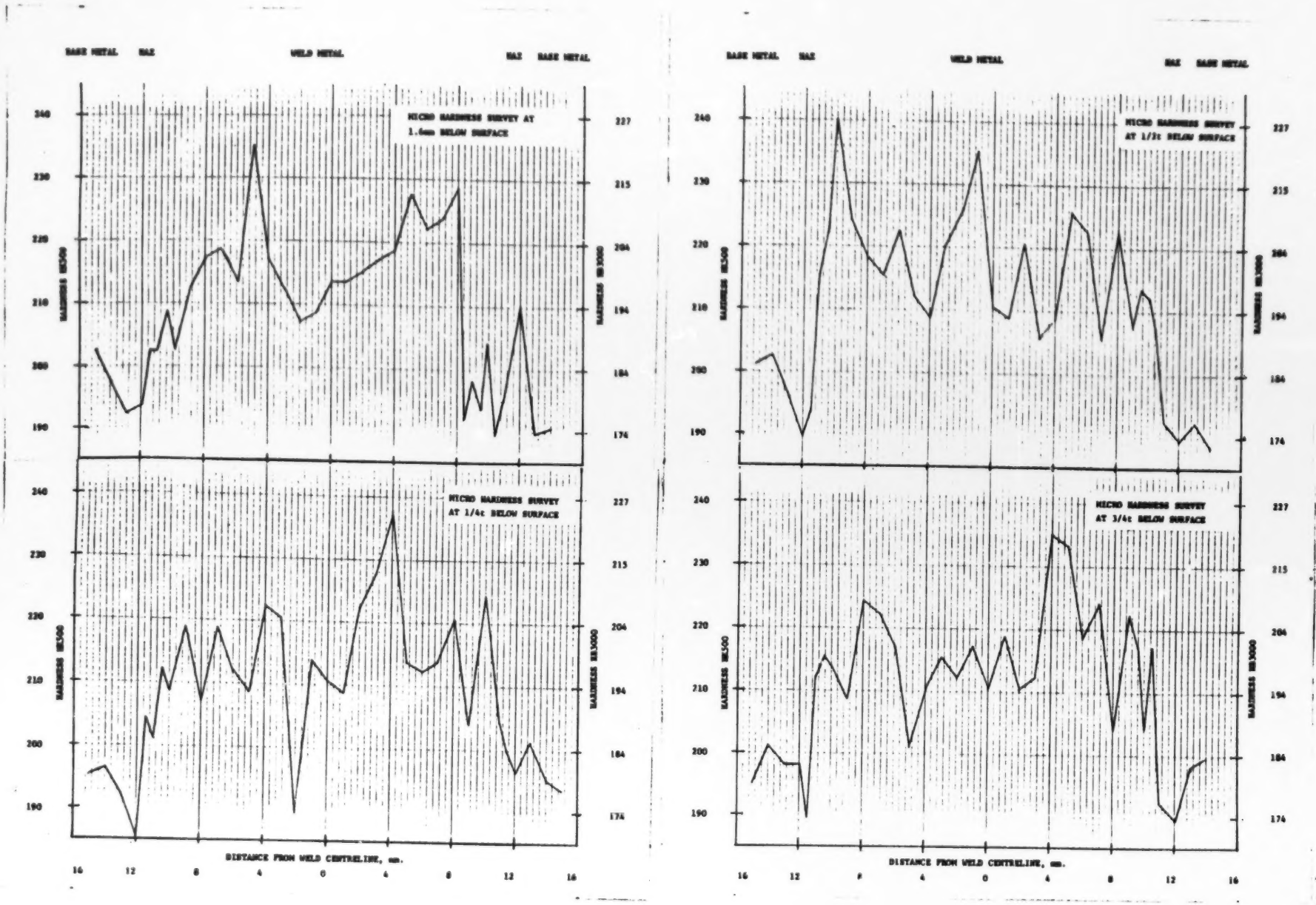

FIGURE 24: MICRO HARDNESS SURVEY THROUGH FULL THICKNESS WELD